The completion of this thesis
was supported by the
Randy Seeling Award
given, in his memory, to another
outstanding graduate student
of the Geology Department,
University of Minnesota, Duluth.

PETROGRAPHY AND DIAGENESIS OF THE UPPER CAMBRIAN MT. SIMON SANDSTONE, SOUTHEASTERN MINNESOTA

A THESIS
SUBMITTED TO THE FACULTY OF THE GRADUATE SCHOOL
OF THE UNIVERSITY OF MINNESOTA
BY

RUBEN DARIO URIBE A.

IN PARTIAL FULFILLMENT OF THE REQUIREMENTS
FOR THE DEGREE OF
MASTER OF SCIENCE

JUNE, 1994

ABSTRACT

The Mt. Simon Sandstone (or Mt. Simon Formation) is the lowermost formation of the Dresbachian Stage (Upper Cambrian). The unit rests unconformably on a wide variety of Precambrian rocks in southeastern Minnesota and its average thickness is near 260 feet. The Mt. Simon Sandstone is dominantly a white to gray, medium- to fine-grained quartz sandstone ($Q_{95.4}F_{4.1}L_{0.5}$) with minor intercalated thin shale beds. A noticeable feature of the unit is the abundance of authigenic potassium feldspar.

Petrography and microprobe analysis were used to identify the framework and matrix constituents of the Mt. Simon Sandstone and to determine the diagenetic textures, paragenetic sequence and chemical composition of authigenic feldspars.

Almost 95 percent of the framework grain components consist of monocrystalline (common) quartz, potassium feldspar and plagioclase, with the feldspar content higher in finer sandstones. Other minor detrital minerals include polycrystalline quartz, vein(?) quartz, recycled quartz, rock fragments, micas, collophane fossil fragments (brachiopods), and glauconite.

Potassium feldspar is the most common authigenic mineral in the Mt. Simon Sandstone. The feldspar is present in almost all the samples as euhedral to subhedral overgrowths on detrital grains, ranging from 0.2 to 23.5 percent. The overgrowths are not in optical continuity with the detrital cores, and are usually pure orthoclase in composition, as evidenced by electron microprobe analysis. Minor quartz cement is present along detrital quartz contacts and in very few cases as obvious overgrowths. Authigenic dolomite exhibits two different textures: a) As euhedral, sand-sized rhombic crystals with considerable zonation showing iron-rich (red) and iron-poor dolomite (clear), and b) As rhombic finely crystalline subhedral crystals replacing illitic matrix. Poikilotopic calcite is found in a few samples, partially replacing detrital and authigenic minerals. Calcite is also present as isolated patches filling pore spaces. Kaolinite cement is most commonly found as vermicular aggregates filling pore spaces. Other authigenic minerals include hematite, pyrite and leucoxene, present as grain coatings and pore fillings.

A high mineralogical maturity in the sandstones is evidenced by the presence of rounded to subrounded zircon, tourmaline, garnet and rutile. Other non-opaque detrital

heavy minerals found include apatite, amphibole, pyroxene, epidote, diaspore and staurolite.

The sandstone has undergone a varied diagenetic history, which includes precipitation and dissolution of authigenic minerals, dissolution of unstable detrital grains, and compaction. The paragenetic sequence in the Mt. Simon can be summarized in three stages: an early diagenesis stage marked by the presence of leucoxene and iron oxides; a burial diagenesis stage marked by the precipitation of quartz, potassium feldspar, kaolinite, illite, dolomite and siderite(?); and finally a late diagenetic stage which includes pyrite and calcite. The total average porosity for all samples is 15.5 percent; part of it is secondary porosity, as evidenced by the presence of partially dissolved grains, cements and matrix.

ACKNOWLEDGEMENTS

I would like to acknowledge all the people who helped me to complete this thesis. The invaluable advice and guidance of Dr. Richard W. Ojakangas who repeatedly read and reviewed the manuscript; his interest, not only in this project but also at all times throughout my stay at the University of Minnesota-Duluth will always be greatly appreciated. I would also like to thank the committee members Dr. Charles L. Matsch and Dr. Dianne Dorland for their suggestions and revisions to the manuscript, Dr. Penelope Morton for providing instruction in the use of the electron microprobe, the Geology Department for partial funding of this project, and all of its faculty and staff members. Dr. G. B. Morey from the Minnesota Geological Survey suggested the problem on which this thesis is based, and the M.G.S. provided all the thin sections. The Minnesota Department of Natural Resources, Division of Minerals Drill Core Library at Hibbing, Minnesota provided the samples for this study. Mark Severson of the Natural Resources Research Institute (NRRI) is thanked for his assistance in operating the electron microprobe. My fellow graduate students at the University of Minnesota-Duluth are thanked for their support and criticisms. My great friend Ann E. Olesen, who will always be in my heart, provided invaluable repeated proofreading of the thesis. Finally I would like to thank very specially my parents for their financial and moral support, as well as my brother and sisters for their continuous encouragement throughout all these four years in the United States.

TABLE OF CONTENTS

ILLUSTRATIONS

PLATES

TABLES

APPENDICES

CHAPTER I

INTRODUCTION

The Mt. Simon Sandstone (or Mt. Simon Formation) is recognized in many places across the North-central states (West Virginia-Nebraska), as a widespread, sheet-like sandstone of Late Cambrian age. The unit rests unconformably on a wide variety of Precambrian rocks. It is dominantly a white to gray, medium-grained quartz sandstone with sporadic thin interlayered shale beds. A noticeable feature of the unit is the abundance of authigenic potassium feldspar. The presence of K-feldspar may be correlated with mineralization of midcontinent Mississippi Valley type lead-zinc deposits. Feldspar authigenesis and ore mineralization could have occurred at the same time by a brine migration event, a result of tectonically expelled fluids from orogenic belts. Other hypotheses that could help to explain the abundance of authigenic feldspar are: a) The presence of alkaline-hypersaline brines developing during late stages of continental denudation and under appropriate climatic conditions (aridity), such as the present lake systems in southern Australia (Long and Lyons, 1992); or b) In-situ framework grain dissolution and subsequent precipitation. Any combination of these three hypotheses could produce the authigenic potassium feldspar.

Purpose of the study:

Specific objectives of this study are to:

a) Integrate petrographic observations and chemical data from five drill cores throughout Southeastern Minnesota in order to determine the diagenetic history of the

unit.

b) Integrate existing information about feldspar authigenesis in sandstones including a bibliographic index of the most significant papers on this topic.

c) Determine the presence, mineralogy and abundance of detrital and authigenic feldspar in the sandstone.

d) Establish textural criteria for the recognition of primary and secondary porosity.

e) Study the heavy mineral suite to determine the mineralogical maturity of the sediments and classify the unit as a first cycle or a multicycle sandstone.

This investigation did not include stratigraphic or sedimentological studies on the Mt. Simon Sandstone, since several works have covered these topics in the past. Among the most important are: Asthana (1969), who presented a complete summary of studies on the Mt. Simon Sandstone prior to 1969; Austin (1969, 1972); Webers (1972); Kiester (1976); Driese and others (1981); Cottingham (1990); and Mossler (1987, 1992).

Location of the study area:

The Mt. Simon Sandstone is poorly exposed in eastern and southeastern Minnesota. Considerable outcrop area can be seen in west-central Wisconsin near the towns of Eau Claire (type section location), Chippewa Falls and Black River Falls. Due to the nature of the study, samples were taken from five drill holes throughout the southeastern part of the state (Fig. 1). Their locations, ground elevations,

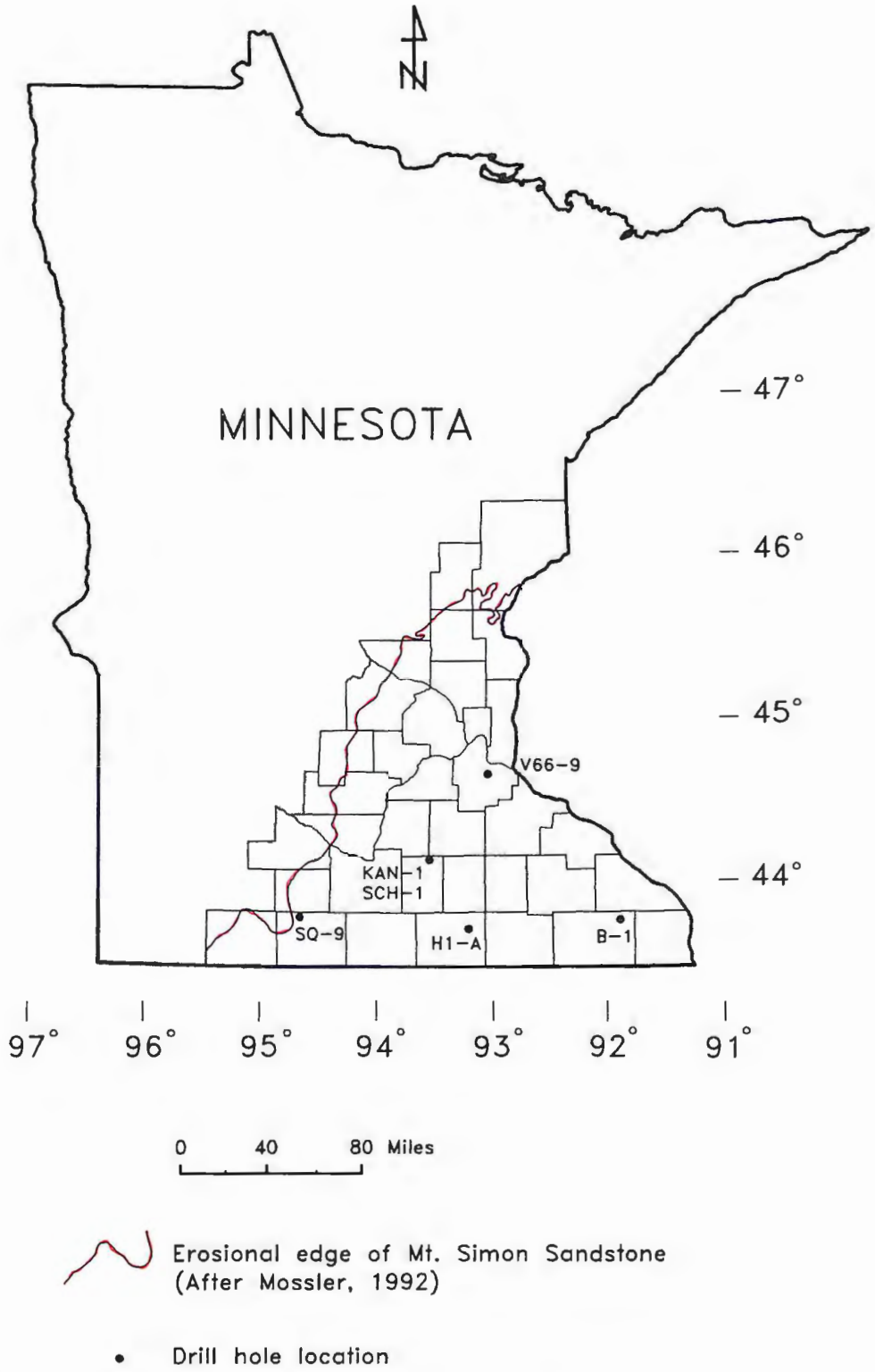

Fig 1: Location map of the study area.

depths and the intervals in which the Mount Simon appears are shown below:

DH= Drill hole L= Location C= County
GE= Ground elevation D= Depth
MSI= Mt. Simon Interval

DH= Northern Natural Gas Hollandale 1-A **(H1A)**
L= SE1/4SE1/4SW1/4 sec. 7, T. 103N., R. 19W.
C= Freeborn
GE= 1202 ft.
D= 1905 ft.
MSI= 1437 - 1619 ft. (182 ft.)

DH= New Jersey Zinc **B-1**
L= NW1/4SW1/4 sec. 25, T. 104N., R. 9W.
C= Fillmore
GE= 800 ft.
D= 1124 ft.
MSI= 407 - 724 ft. (317 ft.)

DH= Pan Ocean Oil, Ltd. **SQ-9**
L= SE1/4SW1/4 sec. 1, T. 104N., R. 32W.
C= Martin
GE= 1185 ft.
D= 703 ft.
MSI= 462 - 686 ft. (224 ft.)

DH= Minnegasco **KAN-1**
L= SE1/4SW1/4SW1/4 sec. 4, T. 108N., R. 22W.
C= Waseca
GE= 1119 ft.
D= 1170 ft.
MSI= 868 - 1169 ft. (301 ft.)

DH= Minnegasco **SCH-1**
L= NW1/4NE1/4 sec. 6, T. 108N., R. 22W.
C= Waseca
GE= 1118 ft.
D= 2080 ft.
MSI= 868 - 1169 ft. (301 ft.)

DH= Northern Natural Gas Vermillion 66-9 **(V66-9)**
L= NW1/4NW1/4 sec. 11, T. 114N., R. 18W.
C= Dakota
GE= 900 ft.
D= 950 ft.
MSI= 635 - 920 ft. (285 ft.)

A composite log of drill holes KAN-1 and SCH-1 was made due to part of the cores being missing; the wells are 1.7 miles apart and were drilled almost at the same ground elevation.

Methods of study:

A total of 105 random samples were collected at the Minnesota Department of Natural Resources, Division of Minerals drill core library, at Hibbing Minnesota. A total of 95 thin sections from the Mt. Simon Sandstone was analyzed for diagenetic textures and mineralogy using a petrographic microscope. The thin sections were impregnated with blue epoxy to show porosity, and were stained for potassium with sodium cobaltinitrite to distinguish K-feldspar from untwinned plagioclase and in some instances from quartz. All the thin sections were point counted. One hundred equally spaced points on each of 6 random traverses were counted for a total of 600 points per thin section. Volume percentage of each mineral and porosity were

tabulated on a spreadsheet.

Several samples were prepared for electron-microprobe analysis by making polished thin sections from the already cut heels. Microprobe analysis helped to determine quantitative chemical composition of feldspar cores and overgrowths, as well as dolomite and calcite compositions.

Twenty representative samples from four drill holes were selected and heavy mineral mounts were prepared for each one using sodium polytungstate heavy liquid (Density = 2.8 g/cm^2). A total of 300 non-opaque heavy minerals were identified and counted in each of 11 grain mounts using the petrographic microscope. Heavy mineral percentages were tabulated on a spreadsheet for further analysis.

Visits to outcrops of the Mt. Simon and the underlying older Precambrian rocks in west-central Wisconsin were made in order to better understand and compare some of the features seen in the drill holes from southeastern Minnesota.

Previous work:

Most of the previous studies on the petrography and diagenesis of Cambrian sandstones have been in the Illinois basin. Ojakangas (1963) study the petrology and sedimentation of the Upper Cambrian Lamotte Sandstone of Missouri. The Lamotte Sandstone in Missouri and the Mt. Simon Sandstone in Minnesota are correlative since both units were deposited by the same transgressive sea, upon Precambrian rocks during Upper Cambrian time. The author concluded that tourmaline-bearing Precambrian sandstones in the Lake Superior region were probably the principal source

for the Lamotte Sandstone in Missouri. His work is the only comparable petrographic study of an Upper Cambrian sandstone unit in the Midcontinent region. Metarko (1980) explained systematic relationships among grain fabric types, cements, primary and secondary porosity and water chemistry of the Mt. Simon and Lamotte Sandstones. Hoholick and others (1984), described variations of cements and porosity types in the St. Peter and Mt. Simon Sandstones. Fishman (1992) discussed the importance of diagenetic studies on the paleohydrology on the Mt. Simon Sandstone.

Other works on a more regional level (Upper North American Midcontinent) have been completed. Heald and Larese (1973) described the importance of post-depositional solution of feldspar as a significant process in porosity development in the Mt. Simon Sandstone of West Virginia and Ohio. Odom (1975) and Odom and others (1976), emphasized the significance of feldspar distribution (abundance) among different size fractions of Cambrian quartz-rich sandstones of the Upper Mississippi Valley. Duffin (1990) in his Ph.D. thesis described the potassic alteration of Cambrian-Ordovician sandstones, and in particular the potassic diagenesis of the Mt. Simon Sandstone in Wisconsin, Iowa, Illinois, Missouri, Indiana, and Ohio.

Local studies (southeastern Minnesota) on petrography and diagenesis of Cambrian units are scarce. Graham (1930) introduced the importance of textural and petrographic studies (grain size distribution and shape, mineralogy of light and heavy fractions, overgrowths, inclusions, etc.), as an alternative tool for stratigraphic correlations in Cambrian sandstones of Minnesota where fossils or other stratigraphic indicators were not present. Tester and Atwater (1934) in their paper on the occurrence of

authigenic feldspar in sediments, mentioned the importance of different types of secondary feldspar in differentiating uppermost Keweenawan formations of Northeastern Minnesota from the Mt. Simon. Goldich (1934) studied authigenic feldspars, chiefly in the New Richmond Sandstone (Lower Ordovician) of southeastern Minnesota. Kiester (1976) in his master's thesis described the texture and mineralogy of the Cambrian strata of southeastern Minnesota. The most recent study is by Mossler (1992) who briefly described the petrography of the Dresbachian age (Late Cambrian) rocks. He also delineated in detail the lithofacies and paleogeographic interpretations for the Dresbachian stratigraphic sequence (Mt. Simon Sandstone, Eau Claire Formation and Galesville Sandstone). His work was a valuable background for this study.

CHAPTER II

REGIONAL GEOLOGY AND LITHOSTRATIGRAPHY

Precambrian Basement Framework:

Cambrian rocks in the central Midcontinent are underlain by Archean and Proterozoic igneous, sedimentary and metamorphic rocks, representing a marked unconformity recognized throughout the northern Midcontinent region. Precambrian rocks in this area have undergone several episodes of deformation. The latest of these episodes is the formation of the Midcontinent rift during Keweenawan time, 1.1 billion years ago. This rift system, also called the midcontinent gravity high, is a very prominent gravity anomaly that extends in a northeast trend from northern and eastern Kansas, through southeast Nebraska, central Iowa, eastern Minnesota, into Lake Superior. It also extends from Lake Superior southeastward into Michigan. Thick piles of basalt and sediments, intruded by mafic bodies, make up most of the rift. Structural features in Cambrian rocks are thought to be the continuation of structural activity along the Precambrian basement structures associated with the Midcontinent rift system (Bunker and others, 1988). A few Precambrian positive elements in the midcontinent area were the source for Cambrian sediments, including the Wisconsin dome, the Transcontinental arch, and the Sioux ridge.

Cambrian Chronostratigraphy:

Rocks of Early Paleozoic age in southeastern Minnesota were deposited in a shallow depression called the Hollandale Embayment (Austin, 1969). The embayment extended northward from the Forest City basin (Iowa basin) into southeastern

Minnesota and southwestern Wisconsin (Fig. 2). During Dresbachian time (lower stage of the St. Croixan Series or earliest Late Cambrian), a major transgression and regression are reported (Lochman-Balk, 1970). The first Late Cambrian transgression of the craton deposited the Mt. Simon Sandstone and the Eau Claire Formation over Precambrian basement during Early and Middle Dresbachian time. During this event, marine and marginal marine waters inundated the craton, including major depocenters such as the Illinois and Iowa basins, and marginal areas such as the Hollandale embayment (Mossler, 1992). During Late Dresbachian (time of maximum regression), Early and Middle Dresbachian deposits were exposed as a flat coastal plain with scattered hills of resistant Precambrian rocks (Lochman-Balk, 1970). This event is recorded by the coarse detrital sediments of the Galesville Sandstone (Mossler, 1992). A second Late Dresbachian transgression marked the beginning of the Franconian Stage. Marine waters at this time occupied almost the same areas covered during Early-Middle Dresbachian transgressions (Lochman-Balk, 1970).

Dresbachian lithostratigraphy and depositional environments:

As mentioned before, the Dresbachian Stage of southeastern Minnesota is composed of the Mt. Simon Sandstone, the Eau Claire Formation and the Galesville Sandstone (Fig. 3).

Mt. Simon Sandstone:

The Mt. Simon Sandstone consists mainly of medium- to coarse-grained quartz sandstone with minor interbedded shale, fine-grained quartz sandstone and conglomeratic

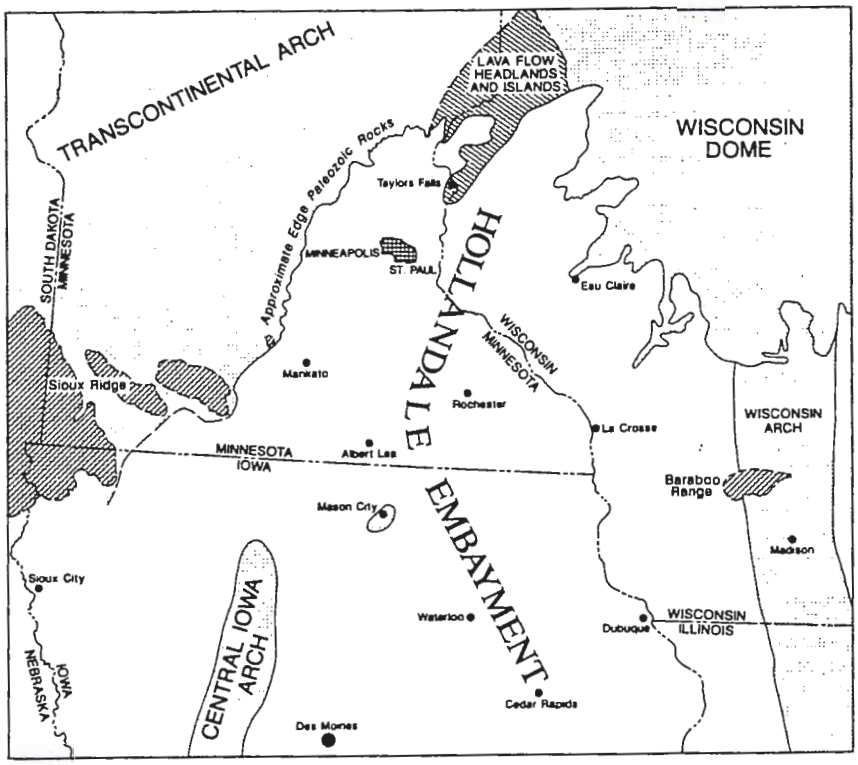

Fig. 2: Paleogeography of southeastern Minnesota and adjoining areas during Upper Cambrian (From Mossler, 1992).

			Formation	Member
LATE CAMBRIAN	ST. CROIXAN SERIES	DRESBACHIAN STAGE	GALESVILLE SANDSTONE	
			EAU CLAIRE FORMATION	SANDY UNIT
				SHALY UNIT
				GREENSAND UNIT
				DOLOSTONE UNIT / SAND/SHALE UNIT
				RED UNIT
			MT. SIMON SANDSTONE	Upper
				Middle
				Lower

Fig. 3: Late Cambrian stratigraphic nomenclature for Minnesota. (After Mossler, 1987 and 1992).

sandstone. In most cases, it is moderately to well sorted; grains are predominantly rounded to well rounded in the medium- to coarse-grained fractions and subrounded to angular in the finer fractions (<0.125 mm). Quartz is the main detrital mineral together with feldspar which reaches high percentages in the fine- to very fine-grained sandstones. Further mineralogical analysis based upon petrographic research in the unit will be discussed in detail in a separate chapter. The Mt. Simon Sandstone is interpreted to have been deposited in a shallow-water high-energy environment (Austin, 1970). The different lithofacies present in the unit were interpreted by Mossler (1992) as follows:

- Basal conglomerate: Braided fluvial deposit.

- Medium- to coarse-grained sandstone (Lower Mt. Simon): Braid plain, braid delta, and littoral deposits.

- Fine- to medium-grained sandstone and shale beds (Middle Mt. Simon): Distal braid delta deposits.

- Upper Mt. Simon sandstone: Sand shoals and tidal flat deposits.

Several other subfacies not mentioned here were described by Mossler in his study.

Eau Claire Formation:

This consists of four different lithofacies in Minnesota. It was described, from the lowest to the upper unit, by Austin (1970) as follows:

- Bioturbated red silty sandstone (red unit).
- Glauconitic sandstone (green sand unit).
- Interbedded shale and fine-grained sandstone (shaly unit).
- Fine-grained sandstone with some interlayered grayish-green shale (sandy unit).

The Eau Claire Formation is interpreted to have been deposited in a shallow sea (Austin, 1970). Mossler (1992) provided a more detailed paleoenvironmental interpretation for the lithofacies mentioned above.

Galesville Sandstone:

The Galesville Sandstone in Minnesota, as described by Austin (1969) is a white to light gray, slightly glauconitic, well to moderately sorted sandstone. It is mostly medium-grained except at the base where fine-grained sandstone beds are present. Sediments of the Galesville Sandstone are interpreted as foreshore, shoreface and tidal channel deposits, which indicate a marine transgression (Mossler, 1992).

CHAPTER III

PETROGRAPHY

Ninety-five thin sections from drill core samples of the Mt. Simon Sandstone were analyzed. One hundred equally spaced points on each of six random traverses (perpendicular to the bedding) were counted for a total of 600 points per thin section. All thin sections were prepared with blue epoxy to easily identify pore spaces. Staining for potassium feldspar (using sodium cobaltinitrite) was also done on all thin sections to distinguish K-feldspar from untwinned plagioclase and quartz.

A few samples show thin (3 to 5 mm) lenses and\or layers of silt- and clay-sized material. These layers and lenses were ignored during point counting and in these cases an extra traverse was chosen to expand the number of points to 600.

Table 1 shows the petrographic summary for the Mt. Simon Sandstone in each of the five drill holes chosen for this study (Fig. 1).

OPERATIONAL DEFINITIONS:

Following is a description of the rock-forming minerals in the Mt. Simon Sandstone as seen in thin section. The abbreviations shown for each constituent are used in Table 1.

Framework grains:

Common quartz (CQTZ): Single crystals with straight to

	QUARTZ					FELDSPAR				ROCK FRAGMENTS				MICA		
SAMPLE #	CQTZ	PQTZ	VQTZ	RQTZ	TOT.QTZ	ORTH	MICR	PLAG	TOT.FEL	PRF	SRF	SQRF	TOT.RF	MUSC	BIOT	MATRIX
RU-H1A-1443	33.5	X			33.8	4.8	2.2	0.5	7.5							
RU-H1A-1454	53.7	0.5			54.2	2.8	1.3		4.2							
RU-H1A-1464	53.5	X			53.7	2.0	1.7	X	3.8					0.5		
RU-H1A-1485	70.2	0.5	X		71.0		X	X	0.3							
RU-H1A-1499	73.3	0.5			73.8	X	0.7		1.0							
RU-H1A-1507	72.7	1.5			74.2											
RU-H1A-1510	69.2	0.5			69.7	2.5	1.0	X	3.8					X		
RU-H1A-1515	65.8	1.0			66.8	1.3	X	X	2.0							
RU-H1A-1522	58.0	3.5			61.5	3.0	1.3		4.3							
RU-H1A-1527	69.7	2.7			72.3	1.2	0.7	X	2.2					1.7		
RU-H1A-1583	55.5	2.2			57.7	2.5	1.0	0.7	4.2					0.8		
RU-H1A-1585	51.3	1.3	X		52.8	4.0	2.0	0.5	6.5					X		
RU-H1A-1589	53.4	7.8	X		61.5		0.5	3.7	4.2							
RU-H1A-1608	47.4	0.7	X		48.5	7.5	2.3	1.3	11.2					3.2		
RU-H1A-1617	59.5	1.5	X		61.2	3.0	X		3.3							
RU-H1A-1619	62.2	7.5	X		70.0	0.5	X	X	1.0							
RU-B1-409	69.3	0.5	X		70.0	X		0.8	1.0							1.7
RU-B1-414	61.5	X	0.8		62.7	2.2	X	3.2	5.7							
RU-B1-419	74.2	X	X		74.8			X	0.2							
RU-B1-437	46.2	X			46.5	5.0	0.7	7.0	12.7					0.7		8.8
RU-B1-441	53.2	1.5	0.5		55.2	2.7	0.5	4.8	8.0					X		8.5
RU-B1-450	72.5	3.0	2.5		78.0	1.0	X	3.2	4.5							
RU-B1-469	74.7	1.5	X		76.5			0.7	0.7							0.8
RU-B1-474	64.3	1.3	X		65.8	2.0	X	3.3	5.5					X		
RU-B1-488	71.0	1.3	0.8		73.2			0.8	0.8	0.7			0.7			
RU-B1-507	70.7	1.3			72.0	0.7	X	3.2	4.0							
RU-B1-523	69.5	2.3	1.5		73.3	X		0.5	0.7		1.0		1.0			
RU-B1-537	61.7	2.3	1.7		65.7	1.8	0.7	3.0	5.5							
RU-B1-562	49.3	1.2	1.0		51.5	3.5	0.7	6.8	11.0							
RU-B1-598	46.5	X			46.8	5.7	X	6.8	12.8	X			0.2	X	1.3	12.7
RU-B1-626	67.0	3.3	1.5		71.8	X		1.0	1.3	X			0.2			
RU-B1-657	64.2	1.7	0.8		66.7	1.5	X	3.8	5.7	0.7			0.7	X	X	
RU-B1-671	62.0	1.7	1.2		64.8	2.2	X	3.8	6.2					X		
RU-B1-682	59.3	1.2	0.7		61.2	4.0	1.0	3.7	8.7						X	
RU-B1-695	61.2	1.3			62.5	3.3	0.8	2.7	6.8							
RU-B1-709	62.8	1.3	1.5		65.7	1.2	0.5	2.0	3.7	X			0.2			
RU-B1-718	55.7	6.2	1.8		63.7	3.2	0.5	3.5	7.2	1.2			1.2	X		X

Table 1: Petrographic summary of the Mt. Simon Sandstone. Sample numbers give drill hole name (abbreviated), and footage in the core. Drill hole locations are shown in Figure 1.

ABBREVIATIONS:

CQTZ: Common quartz
PQTZ: Polycrystalline quartz
VQTZ: Vein (?) quartz
RQTZ: Recycled quartz
ORTH: Orthoclase
MICR: Microcline
PLAG: Plagioclase
PRF: Plutonic rock fragments
SRF: Siltstone rock fragm.
SQRF: Sioux Quartzite rock fragments
MUSC: Muscovite
BIOT: Biotite
QTZ: Quartz (Cement)
FELD: Feldspar
DOL: Dolomite
CAL: Calcite
SID: Siderite
KAOL: Kaolinite
ILL: Illite ?
PY: Pyrite
HEM: Hematite
LEUC: Leucoxene
COLL: Collophane
PYRE: Pyrite replaced shells
GLAU: Glauconite
Q: Quartz
F: Feldspar
L: Lithics (Rock fragments)
QTZSS: Quartz sandstone
FLDSS: Feldspathic sandstone
SLTSS: Sublithic sandstone

CEMENT										FOSSILS				CLASSIFICATION			
QTZ	FELD	DOL	CAL	SID	KAOL	ILL (?)	PY	HEM	LEUC	COLL	PYRE	GLAU	PORES	Q	F	L	RNAME
6.2	23.5		1.0					1.0	0.7	1.5			24.8	81.9	18.1		FLDSS
6.3	14.5							X	1.3	X			19.0	92.9	7.1		FLDSS
4.3	17.3							3.2	0.7	1.8			14.7	93.3	6.7		FLDSS
6.8	1.2							X	X	1.0			19.2	99.5	0.5		QTZSS
4.5	3.5				0.5			0.8	2.2	2.0			11.7	98.7	1.3		QTZSS
5.2	0.8	3.8											16.0	100.0			QTZSS
4.3	10.0							2.0		X			9.8	94.8	5.2		FLDSS
4.7	3.0	3.5											20.0	97.1	2.9		QTZSS
2.5	10.5	9.8						1.2					10.2	93.4	6.6		FLDSS
2.0	8.3	4.2						1.0					8.3	97.1	2.9		QTZSS
4.0	12.5				0.5			8.0					12.3	93.3	6.7		FLDSS
3.2	13.0				2.0			0.7					21.5	89.0	11.0		FLDSS
2.2	8.0								3.2				23.0	93.7	6.3		FLDSS
1.0	18.7				4.0			2.8					10.7	81.3	18.7		FLDSS
3.0	6.7				1.2				4.7				20.0	94.8	5.2		FLDSS
1.5	6.2								8.8				12.5	98.6	1.4		QTZSS
1.7	2.0						2.7			1.7	1.2		18.2	98.6	1.4		QTZSS
3.0	4.0						1.3			1.8	1.0		20.5	91.7	8.3		FLDSS
2.0	X						1.2			X			21.3	99.8	0.2		QTZSS
2.0	8.7						2.0						18.7	78.6	21.4		FLDSS
1.5	8.8						2.0						17.7	87.3	12.7		FLDSS
1.2	3.3						0.5						12.5	94.5	5.5		FLDSS
1.7	1.8						1.8						16.7	99.1	0.9		QTZSS
1.7	7.0						2.0						17.8	92.3	7.7		FLDSS
2.0	2.3						1.8						19.2	98.0	1.1	0.9	QTZSS
2.3	4.0						2.7						15.0	94.7	5.3		FLDSS
1.3	1.5						1.7			X	X		20.2	97.8	0.9	1.3	QTZSS
3.2	6.8						1.8						17.0	92.3	7.7		FLDSS
1.8	9.5										0.8		25.3	82.4	17.6		FLDSS
2.0	8.3						0.7						13.0	79.0	20.8	0.3	FLDSS
1.7	1.5		1.2										22.3	98.0	1.8	0.2	QTZSS
2.3	5.3		X				1.7						17.2	91.3	7.8	0.9	FLDSS
1.8	7.0		1.8				0.2						17.8	91.3	8.7		FLDSS
1.0	7.0		X										21.7	87.6	12.4		FLDSS
2.7	6.3		2.7				0.5						18.5	90.1	9.9		FLDSS
1.7	4.5		4.2				0.8						19.3	94.5	5.3	0.2	FLDSS
1.5	7.0		5.5				1.0						12.3	88.4	10.0	1.6	FLDSS

X = Trace amount (Less than 0.5 percent)

Table 1. (Continued)

	QUARTZ					FELDSPAR				ROCK FRAGMENTS				MICA		
SAMPLE #	CQTZ	PQTZ	VQTZ	RQTZ	TOT.QTZ	ORTH	MICR	PLAG	TOT.FEL	PRF	SRF	SQRF	TOT.RF	MUSC	BIOT	MATRIX
RU-SQ9-474	48.8	1.0	0.5	7.1	56.4											
RU-SQ9-483	47.5	X	X	4.0	52.0											
RU-SQ9-545	52.4	2.2	1.3	7.4	63.3							X	0.3			
RU-SQ9-554	49.6	0.8	0.4	4.5	55.3	X			0.2							
RU-SQ9-570	26.7			2.9	29.6	2.2			2.2					0.5		12.5
RU-SQ9-575	25.0			2.0	27.0	4.0		X	4.2							13.0
RU-SQ9-595	51.3	2.2	2	9.3	64.8											
RU-SQ9-630	56.4	3.0	3.9	4.0	67.3											
RU-SQ9-647	59.0	2.2	3.5	4.5	69.2	0.8			0.8							12.3
RU-SQ9-652	55.5	3.5	1.2	3.2	63.4	0.5			0.5							29.2
RU-SQ9-654	64.3	2.8	0.8	5.5	73.4	0.5		X	0.7			X	0.2			
RU-SQ9-666	57.8	2.8	1	7.2	68.8	1.5			1.5			X	0.2			
RU-SQ9-669	50.1	5.2	4	4.9	64.2							1.2	1.2			
RU-SQ9-672	54.6	5.7	3.6	7.6	71.5							1.0	1.0			
RU-SQ9-677	51.8	12.8	5	3.3	72.9							4.3	4.3			
RU-SQ9-678	58.4	2.5	3.1	8.4	72.4											
RU-SQ9-681	56.2	3.3	2.8	7.4	69.5											
RU-SQ9-686	55.5	6.3	1.2	1.5	64.5							4.3	4.3			
RU-SCH-869	45.5				45.5	X		X	0.5		1.2		1.2			
RU-SCH-874	71.2				71.2	X		0.5	0.8		2.3		2.3			
RU-SCH-881	62.7				62.7	0.7		0.8	1.5							
RU-SCH-897	46.5				46.5	6.0	0.5	3.0	9.5							14.2
RU-SCH-909	64.2		4.5		68.7			X	0.2							1.5
RU-SCH-926	67.5	0.8			68.3	3.3	0.7	2.3	6.3							0.8
RU-SCH-930	76.2	0.7	1.7		78.5	X		X	0.3							
RU-KAN-923	30.8				30.8	3.7		1.2	4.8							
RU-KAN-938	38.7				38.7	4.8		2.5	7.3							3.8
RU-KAN-948	60.3				60.3	3.0	X	2.0	5.3							
RU-KAN-962	65.0				65.0	X		0.8	1.2		0.5		0.5			
RU-KAN-991	57.7				57.7	X		X	0.3		1.2		1.2			X
RU-KAN-1012	75.2	1.2	2.3		78.7			X	0.2							0.7
RU-KAN-1023	74.3	0.5	1.8		76.7	2.2	X	1.8	4.3							2.0
RU-KAN-1038	74.3	0.5	0.8		75.7	0.5		1.0	1.5							
RU-KAN-1081	74.2	0.5	1.0		75.7											
RU-KAN-1097	74.7	3.5	3.3		81.5			0.8	0.8							
RU-KAN-1140	70.2	3.0	1.7		74.8	X	X	0.7	13	X			0.3			1.8
RU-669-644	61.8	1.7	1.2		64.7	X		X	0.5	X			0.5			
RU-669-653	69.5	3.0	5.0		77.5	X			0.3	0.5			0.5			
RU-669-675	76.3	1.5	0.7		78.5	0.5		1.3	1.8	X			0.2			
RU-669-693	76.0	X	0.8		77.2	X		1.3	1.7							
RU-669-715	74.3	3.7	X		78.3			0.5	0.5	0.5			0.5			
RU-669-726	67.8	6.3	X		74.5	1.2	X	0.5	1.8	1.0			1.0			
RU-669-743	72.3	3.0			75.3			0.7	0.7							
RU-669-770	67.7	5.8			73.5	1.2	X	2.5	4.0							
RU-669-788	70.3	1.2	0.8		72.3	1.3	X	1.0	2.7	X			0.2			
RU-669-799	65.5	5.5	0.7		71.7	X	X	0.7	1.2	X			0.2			
RU-669-809	74.2	4.7	0.5		79.3	0.8		0.5	1.3	1.5			1.5			
RU-669-814	65.5	5.8	0.7		72.0	0.5		1.2	1.7	X			0.3			
RU-669-828	69.8	1.8	0.3		72.0	1.3	0.7	0.5	2.5	X			0.3			
RU-669-838	70.8	2.3	1.3		74.5	0.7		X	1.0							
RU-669-856	64.3	2.7	X		67.2	2.3	1.3	X	4.0	1.7			1.7			
RU-669-867	53.8	4.8	0.5		59.2	3.5	0.7	0.8	5.0	0.5			0.5			
RU-669-885	70.5	1.8	3.5		75.8		X	X	0.3							
RU-669-892	62.2	6.8	5.0		74.0	2.0	X		2.3						X	
RU-669-902	58.5	11.8	4.3		74.7	X			0.2	0.8			0.8			
RU-669-910	58.7	4.7	6.5		69.8	0.5	X	X	1.0	0.7			0.7			
RU-669-914	53.8	9.2	7.5		70.5	1.0	0.5	X	1.7	X			0.2	0.8		
RU-669-920	59.8	2.0	5.0		66.8	3.3	0.7	X	4.3	0.5			0.5		0.5	

CEMENT										FOSSILS				CLASSIFICATION			
QTZ	FELD	DOL	CAL	SID	KAOL	ILL (?)	PY	HEM	LEUC	COLL	PYRE	GLAU	PORES	Q	F	L	RNAME
3.6					15.5								22.5	100.0			QTZSS
2.0			39.8		3.0								3.2	100.0			QTZSS
3.7			0.7		9.2								22.8	99.5		0.5	QTZSS
3.0			29.2		8.5								3.8	99.7	0.3		QTZSS
1.4	3.8	36.2			4.8					2.7			8.3	93.2	6.8		FLDSS
1.0	8.0	15.7	12.0							1.2		10.2	7.8	86.6	13.4		FLDSS
5.1					13.3								16.8	100.0			QTZSS
2.7				7.2	X								22.7	100.0			QTZSS
2.2	X		1.8		2.3								11.0	98.8	1.2		QTZSS
1.8	1.2	X											3.8	99.2	0.8		QTZSS
2.7	X												22.8	98.8	0.9	0.3	QTZSS
3.6					8.5								17.3	97.6	2.1	0.3	QTZSS
2.5		X			24.3			X					7.5	98.2		1.8	QTZSS
3.7		0.7			8.8								14.3	98.6		1.4	QTZSS
1.5					16.5								4.8	94.4		5.6	SLTSS
4.1					6.0								17.5	100.0			QTZSS
3.6			X		X								26.3	100.0			QTZSS
0.8					27.2								3.2	93.8		6.2	SLTSS
	X	16.0						26.2		0.8			9.5	96.5	1.1	2.5	QTZSS
2.3	1.0	2.5						0.5		0.5			18.8	95.7	1.1	3.1	QTZSS
1.0	1.7	8.5						7.5		1.7			17.5	97.7	2.3		QTZSS
2.0	9.3							5.0		X			13.2	83.0	17.0		FLDSS
2.7	0.8							1.8		8.2			16.2	99.8	0.2		QTZSS
1.2	5.0							3.5		X			14.7	91.5	8.5		FLDSS
2.0	1.0							1.3		X			16.7	99.6	0.4		QTZSS
1.7	8.3	8.8								2.2		31.5	11.8	86.4	13.6		FLDSS
2.3	10.7	8.7								1.3		11.3	17.8	84.1	15.9		FLDSS
2.7	5.7	5.2								1.2		4.0	15.7	91.9	8.1		FLDSS
1.7	1.7	8.7						7.5		2.3			11.5	97.5	1.8	0.8	QTZSS
0.5	0.8	11.2						14.2		5.2			8.7	97.5	0.6	2.0	QTZSS
2.8	0.5							1.5		1.7			14.0	99.8	0.2		QTZSS
2.2	4.3							0.5					10.0	94.7	5.3		FLDSS
2.3	2.8							0.3					17.3	98.1	1.9		QTZSS
2.7								3.5		X			17.8	100.0			QTZSS
1.5	1.3							0.3					14.5	99.0	1.0		QTZSS
2.3	2.3							0.8					16.2	97.8	1.7	0.4	QTZSS
1.7	1.0						X			14.7	4.3		12.8	99.0	0.5	0.5	QTZSS
1.8	1.0	X					X						18.3	98.9	0.4	0.6	QTZSS
1.7	3.3												14.5	97.5	2.3	0.2	QTZSS
1.5	3.8						X						15.7	97.9	2.1		QTZSS
1.8	2.2	X					0.5						16.0	98.7	0.8	0.6	QTZSS
1.0	1.2					5.8							14.7	96.3	2.4	1.3	QTZSS
1.5	1.5	0.7											20.3	99.1	0.9		QTZSS
1.2	5.8						X						15.2	94.8	5.2		FLDSS
1.8	3.7	X					0.5						18.7	98.2	3.5	0.2	QTZSS
1.3	1.3					5.8	X						18.2	98.2	1.6	0.2	QTZSS
1.7	1.3					5.7	X						9.0	96.6	1.6	1.8	QTZSS
2.0	2.8					2.0	0.5						18.7	97.3	2.3	0.5	QTZSS
4.3	2.8						0.5						17.5	96.2	3.3	0.4	QTZSS
2.2	2.7		0.7										19.0	98.7	1.3		QTZSS
2.3	3.5		1.3										20.0	92.2	5.5	2.3	FLDSS
1.2	7.5		9.8				1.7						15.2	91.5	7.7	0.8	FLDSS
4.3	2.2					0.7	X						16.3	99.6	0.4		QTZSS
3.0	4.5		0.8				1.5						13.5	96.9	3.1		QTZSS
3.2	X		3.0				0.5						17.3	98.7	0.2	1.1	QTZSS
7.0	1.5		1.7				1.7						16.7	97.7	1.4	0.9	QTZSS
3.0	6.3		2.8		2.7								12.0	97.5	2.3	0.2	QTZSS
4.0	7.0		X			3.0	X						13.5	93.3	6.0	0.7	FLDSS

slightly undulose extinction (< 5° on conventional flat stage) (Plate 1-A). Needle-shaped rutile inclusions are common. Other inclusions such as zircon, biotite and apatite are also present but rare.

Polycrystalline quartz (PQTZ): Composite grains with two or more crystals (Plate 1-B). Included in this category are grains having mostly straight contacts between crystals (the vast majority), grains consisting of slightly sutured, elongated crystals and coarse-grained chert (very scarce). Some grains show authigenic pyrite along the boundaries between the different crystals. Most polycrystalline grains present a cloudy appearance under one polar.

Vein (?) quartz (VQTZ): Grains of this type are usually unit grains showing numerous fluid inclusions giving the grain a distinctive cloudy appearance under one polar. (Plate 1-C).

Recycled quartz (RQTZ): Subangular to subrounded quartz overgrowths are found in the Pan Ocean Oil, Ltd. SQ9 drill hole in which the Mt. Simon Sandstone directly overlies the Sioux Quartzite. Very few grains of this type are present in the other drill holes. (Plate 1-A).

Potassium feldspar: Feldspar grains showing no twinning were counted as orthoclase (ORTH) (Plate 1-D). Grains with cross-hatched twinning were counted as microcline (MICR) (Plate 1-E).

Plagioclase (PLAG): Unstained feldspar grains and grains showing polysynthetic (?) twinning were counted as plagioclase (Plate 1-F). It is important to mention that due to feldspar grain sizes (usually <0.2 mm), the staining

technique was not always 100 percent reliable. Similarly, the determination of twinning on the small grains is unreliable. Therefore, the quantities of orthoclase and microcline versus plagioclase could have been underestimated; that is, the orthoclase and microcline percentages may be slightly higher than is shown on Table 1.

Plutonic rock fragments (PRF): Usually an intergrowth of K-feldspar (microcline and orthoclase) within large quartz crystals (Plate 1-G).

Siltstone rock fragments (SRF): Composed of angular, silt-sized, quartz and minor feldspar and shell fragments. The grains are usually cemented by phosphatic material, and in a few cases by goethite/limonite (?) (Plate 1-H and 2-H). These grains have most likely been locally derived i.e., from within the basin of deposition (intraformational).

Sioux Quartzite rock fragments (SQRF): Observed only in the drill hole Pan Ocean Oil, Ltd. SQ9 (west of the study area) which is located near the Sioux Ridge. Quartz grains and authigenic quartz, diaspore and kaolinite are the main constituents in these locally derived grains (Plate 2-A). Individual detrital diaspore and kaolinite grains were also counted as rock fragments because of their certain origin from the Sioux Quartzite.

Micas: Muscovite (MUSC) and biotite (BIOT) are commonly present in trace ammounts; muscovite prevails over biotite. The grains are commonly elongated and are part of the very fine-grained fractions and thin shalier beds and lenses (Plate 2-B).

PLATE 1

A: Sample RU-669-910. Photomicrograph of common quartz (Cq) and recycled quartz (?) (Rq). Arrows are showing possible abraded quartz overgrowths. Crossed polarizers, 0.8 mm across.

B: Sample RU-H1A-1619. Photomicrograph of common quartz (Cq) and polycrystalline quartz (Pq). Crossed polarizers, 1.5 mm across.

C: Sample RU-669-910. Photomicrograph of common quartz (Cq) and quartz grain with abundant vacuoles or inclusions (Vq). This grain was probably derived from a hydrothermal vein (low-temperature origin). Porosity (Po) is shown in blue. Plain light, 1.5 mm across.

D: Sample RU-B1-437. Photomicrograph of rounded detrital orthoclase grain (Or). Note the lack of twinning and euhedral K-feldspar overgrowth. Crossed polarizers, 0.4 mm across.

E: Sample RU-669-856. Photomicrograph of rounded detrital microcline grain (Mi). Note the typical cross-hatched twinning and K-feldspar overgrowth. Crossed polarizers, 0.4 mm across.

F: Sample RU-H1A-1617. Photomicrograph of rounded detrital plagioclase grain (Pl). Note polysynthetic twinning and subhedral K-feldspar (?) overgrowth. Crossed polarizers, 0.4 mm across.

G: Sample RU-669-653. Photomicrograph of igneous plutonic rock fragment (PRF). Crossed polarizers, 1.5 mm across.

H: Sample RU-SCH-874. Photomicrograph of a locally-derived (i.e., intraformational) siltstone rock fragment (SRF). The grain is composed mainly of quartz grains with some feldspar grains and shell fragments. The grain is cemented by phosphate material. Plain light, 1.5 mm across.

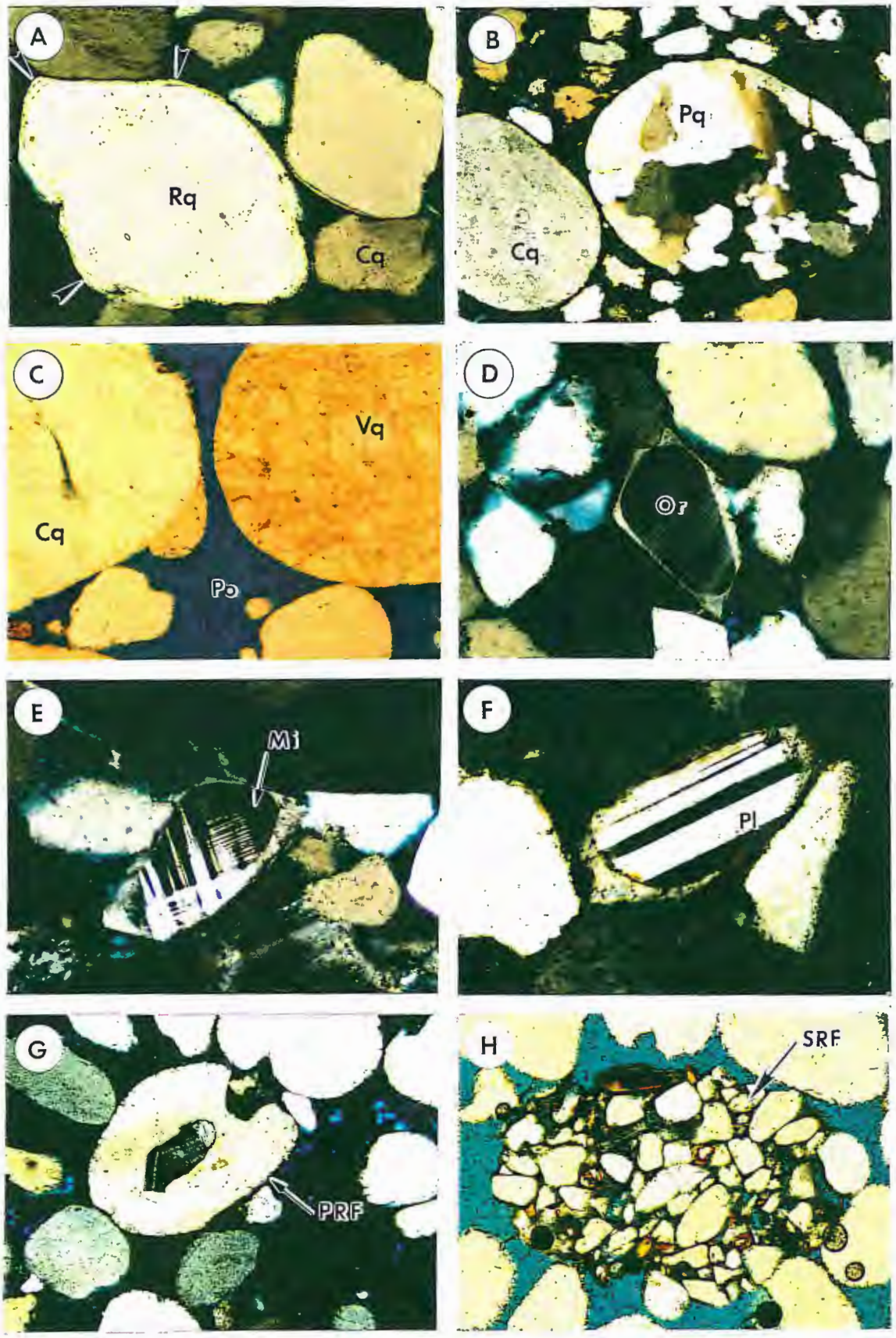
A
Rq
Cq
B
Pq
Cq
C
Vq
Cq
Po
D
Oi
E
Mi
F
Pl
G
PRF
H
SRF

Glauconite (GLAU): Small dark green to yellow-green pellets (up to 0.4 mm) showing an aggregate internal structure of randomly oriented micron-sized crystals (Plate 2-C).

Matrix:

Detrital particles less than 62.5 microns (0.0625 mm) in diameter were considered as matrix. The matrix is syngenetic and apparently has been bioturbated. Very thin clayey layers and lenses (< 2 mm thick) and discontinuous patches or relicts compacted after burial were also considered matrix (Plate 2-D). In some instances these layers and lenses account for up to 29 percent of the rock (RU-SQ9-652) although this fact was not taken into account for the rock classification. Most of the clayey material appears to be potassium-rich (illitic ?), as evidenced by the yellow staining for potassium.

Cement:

Quartz (QTZ): Authigenic quartz was rarely seen as overgrowths. Quartz cement was considered to be present along the boundaries between adjacent quartz grains even though it was not clearly visible as overgrowths.

Feldspar (FELD): Authigenic feldspar is present in almost all of the samples as euhedral overgrowths on detrital feldspar grains. Overgrowths are not in optical continuity with the detrital cores and are usually pure orthoclase in composition.

Dolomite (DOL): Carbonate cement with a distinctive rhombohedral habit was counted as dolomite.

Calcite (CAL): Carbonate cement without any distinctive crystal habit (i.e. anhedral) was counted as calcite. In some cases poikilotopic calcite is found replacing detrital grains and cements, and/or matrix (?), and also filling some pore spaces.

Siderite (SID): Fine rhombohedral-shaped grains are present in only one sample, and appear to be siderite.

Kaolinite (KAOL): Two types of kaolinite cement were found. First, as pore-filling showing a series of large stacked platy crystals or "books" randomly oriented (vermicular kaolinite). Secondly (?), as micron-sized crystals showing a laminae-like structure parallel to bedding.

Illite ? (ILL): Clay-sized oriented crystals usually concentrated around detrital grains. The illitic (?) composition is based only on the yellowish color that this clay presents on thin sections that were stained for potassium.

Pyrite (PY): Commonly anhedral to subhedral masses, brass-yellow in reflected light, and optically opaque.

Hematite (HEM): Hematite-red color in reflected light and optically opaque.

Leucoxene (LEUC): Whitish in reflected light and optically opaque. Present only in the Hollandale H1-A drill hole.

Fossils:

Disarticulated brachiopod shells are usually found in the upper portion of the unit near the contact with the overlying Eau Claire Formation (Plate 2-E & 2-F). Collophane (COLL) is the main constituent of the shells, although in some cases pyrite and rarely hematite, were found replacing part of the shells. Pyrite-replaced shells were counted separately under the category of fossils (PYRE).

DRILL CORE DESCRIPTIONS:

The percentages used in the following descriptions are related to the total rock mineralogy including detrital grains, matrix, cement and pore spaces (see Table 2).

Northern Natural Gas Hollandale 1-A **(H1A)**:

Texture and detrital mineralogy: The most prominent characteristic of the Mt. Simon Sandstone in this location is the grain size. Grains are well-sorted, fine- to very fine-grained sand, except towards the base where moderately sorted very coarse sand levels are present as part of a basal conglomerate. A large number of framework grains are subangular to subrounded. Quartz, most of which is monocrystalline (common quartz), averages 61.4 percent. Feldspar (mostly potassium-rich) ranges from 1 to 11.2 percent (average = 3.7 percent). The feldspar is primarily concentrated in the <0.125 mm sand sizes. Muscovite occurs as fine-grained plates, many of them bent and broken around detrital grains. Broken pieces of brachiopod shells are present in the upper 70 feet, ranging from 0.2 to 1.8 percent in volume.

Authigenic mineralogy: K-feldspar is the most abundant authigenic mineral, ranging from 0.8 to 18.7 percent (average = 9.7 percent). Quartz cement is present along grain boundaries; it ranges from 1 to 6.8 percent (average = 3.9 percent). In order of abundance, after feldspar and quartz, minor quantities (<1.5 percent average) of leucoxene, hematite, dolomite, kaolinite and calcite are present.

Matrix: Sandstones of this locality appear not to contain any matrix, although it is common to find thin layers and lenses of clayey material which were not interpreted as matrix.

Porosity: The average pore space is 15.9 percent.

New Jersey Zinc **B-1**:

Texture and detrital mineralogy: The most noticeable textural feature of the Mt. Simon Sandstone in this location is a marked bimodal distribution of grain size throughout the unit, with each mode well sorted within itself (Plate 2-G). In most cases the mixture consists of rounded to well-rounded coarse sand grains, and subrounded to subangular fine to very fine grains from which the intermediate phase has been selectively removed. A diameter ratio of 5:1 or higher is common between the two grain sizes, with very few grains of intermediate size. Evidence of bioturbation is common, particularly in the upper portion of the unit. The most abundant detrital component is quartz which averages 65.3 percent. Feldspars, mostly plagioclase and orthoclase are present in the finer fractions (<0.125 mm), and average 5.4 percent. Plutonic rock fragments are present toward the bottom half of the unit ranging from 0.2 to 1.2 percent. A

very few grains of phosphate-cemented siltstone are present close to the middle of the unit. Muscovite and minor biotite occur as fine- to medium-grained plates, many bent and broken around detrital grains. Fairly complete but disarticulated shells of brachiopods are present, mainly in the upper 10-15 feet, and range in content from 0.2 to 1.2 percent.

Authigenic mineralogy: K-feldspar, the most abundant authigenic mineral, ranges from 0.2 to 9.5 percent (average = 5 percent). Quartz cement ranges from 1 to 3.2 percent. Pyrite (0.2 to 2.7 percent) is present in almost every sample: a) Cementing detrital grains, b) Along small fractures on the surface of quartz grains and also along crystal boundaries in polycrystalline quartz grains, and c) replacing brachiopod shells. Small amounts of calcite cement are present in the lower part of the unit.

Matrix: Matrix in most cases has been bioturbated. Silty to clayey matrix may also be derived from the removal of material from thin, finely laminated shaly beds and lenses. In both cases the matrix appears to be illitic (?) in composition. The amount of matrix ranges from 0.3 to 12.7 percent (average = 1.6 percent).

Porosity: The average pore space is 18.2 percent.

Pan Ocean Oil, Ltd. **SQ-9**:

Texture and detrital mineralogy: The Mt. Simon Sandstone at this location shows a wide variety of textures. Fine to very fine sands are subangular and well-sorted. Coarser sands are moderately sorted showing better roundness. In some cases, especially toward the base,

bimodal distribution is common but is not as obvious as in the New Jersey Zinc B-1 drill hole. Quartz is the most abundant detrital mineral, averaging 61.5 percent. Apparently most of the quartz grains that make up the unit in this area were derived from the Sioux Quartzite which directly underlies the Mt. Simon in this area. Reworked quartz grains (with visible subrounded to subangular quartz overgrowths ?) range from 1.5 to 9.3 percent. Very coarse, polycrystalline quartz grains including some granules range from 0.2 to 12.8 percent. Quartz grains showing a great amount of inclusions (vein quartz?) are fairly common and range from 0.3 to 3.9 percent. Feldspar, mostly orthoclase, is present in only 7 of 18 samples, ranging between 0.2 and 4.2 percent. Rock fragments from the Sioux Quartzite range from 0.2 to 4.3 percent. Muscovite and a small amount of biotite are present. Close to 10 percent glauconite is present in one of the samples from the middle part of the unit. Brachiopod shells are scarce in this location; they were only found in two samples in the upper part of the unit.

Authigenic mineralogy: Kaolinite cement is found in nearly all samples from the Mt. Simon Sandstone in this location, ranging from 0.2 to 27.2 percent (average = 8.3 percent). Two texturally different types of kaolinite are present; first, as well-crystallized vermicular aggregates in pore spaces and second (?), as micron-sized particles finely laminated around detrital grains, displaying a wavy-looking pattern parallel to the stratification. Toward the top of the unit, two samples are almost totally cemented by poikilotopic calcite crystals; in these cases the average amount of calcite is nearly 35 percent. Calcite is also present in isolated spots filling some of the pores. Dolomite is present as fine (<0.1 mm) subhedral rhomb-shaped

crystals usually replacing illitic (?) clays. Quartz cement is present along quartz grain boundaries. Other minor cements include traces of hematite and what appears to be siderite (present only in RU-SQ9-630); this is yet to be proven by microprobe analysis.

Matrix: The matrix in these rocks has the same characteristics as described in the New Jersey Zinc B-1 drill hole, although in this case clay minerals (illite ?) are partially replaced by dolomite.

Porosity: The average pore space in all the samples is 13 percent.

Minnegasco **SCH-1** and Minnegasco **KAN-1**:

Texture and detrital mineralogy: The Mt. Simon Sandstone in this composite drill-hole shows a wide variety of lithofacies as shown by Mossler (1992). This variety is represented by a number of textures in the sandstone. Among the most common are: a) Well-sorted fine- to very fine-grained sand; b) Moderately sorted medium-grained oolitic sands; c) Moderately to poorly sorted medium-grained sands containing intraformational rock fragments, oolitic grains and brachiopod valves (Plate 2-H); d) Moderately sorted fine-grained glauconitic sands; and e) Abundant interlayered shale beds and lenses (ignored in point counting). Common quartz is the most abundant detrital component (average = 62.7 percent). The amount of feldspar ranges from 0.2 to 9.5 percent and is in most cases, concentrated in the fine- to very fine-grained sand fractions. Intraformational sedimentary rock fragments range from 0.5 to 2.3 percent, and consist of fine-grained siltstone and sandstone, cemented by phosphate and in some cases goethite and\or

PLATE 2

A: Sample RU-SQ9-686. Photomicrograph of Sioux Quartzite rock fragment (SQRF). The grain is composed of quartz (q), kaolinite (k) and diaspore (d). Crossed polarizers, 1.5 mm across.

B: Sample RU-669-920. Photomicrograph showing detrital micas (muscovite = Mu; arrows). Micas are concentrated in the very fine fraction of the sandstones. Crossed polarizers, 1.5 mm across.

C: Sample RU-KAN-923. Photomicrograph of glauconite pellets (G). Rounding does not necessarily indicate abrasion. Plain light, 0.8 mm across.

D: Sample RU-B1-441. Photomicrograph of primary (detrital ?) matrix (M). Matrix is probably related to bioturbation processes. Plain light, 1.5 mm across.

E: Sample RU-KAN-1028. Photograph of brachiopod shells in hand sample. Note the good preservation of the shells.

F: Sample RU-669-644. Photomicrograph of brachiopod shell fragments (B). The original shell material is collophane. Note shells partially replaced by pyrite (Py; arrows). Plain light, 1.5 mm across.

G: Sample RU-B1-562. Photomicrograph showing bimodal grain distribution. The rounded coarse grains are quartz. Finer subrounded to subangular grains are quartz and feldspar (stained yellow). Plain light, 1.5 mm across.

H: Sample RU-SCH-869. Photomicrograph of coated detrital grains. Grains shown are quartz (Q), and a sedimentary rock fragment (SRF). Coatings are of iron oxide, usually hematite. Note shearing of concentric oolitic coating (Oc) (lower right) due to compactional deformation. Grains are partially cemented by carbonate (Ca) (dolomite ?). Plain light, 1.5 mm across.

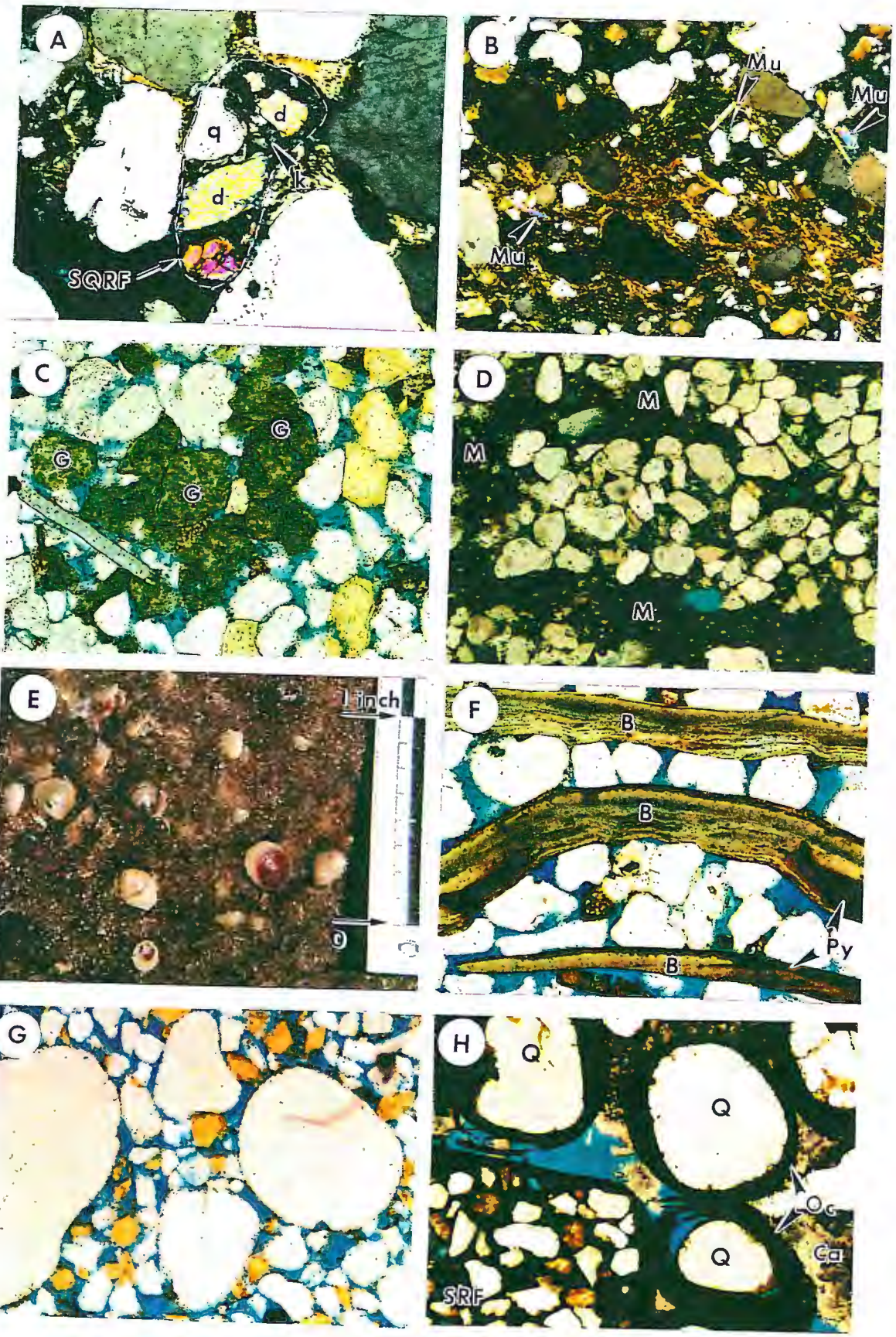
A
q
d
k
d
SQRF
B
Mu
Mu
Mu
C
G
G
G
D
M
M
M
E
1 inch
F
B
B
B
Py
G
H
Q
Q
Q
Oc
Ca
SRF

limonite (?). Glauconite is present in three samples in the upper half of the unit, ranging from 4 to 31.5 percent. Brachiopod valves are present in almost every sample and range from 0.2 to 8.2 percent.

Authigenic mineralogy: Authigenic hematite ranges from 0.3 to 5 percent. It is commonly found as groups of rounded fine, clay-sized specks sometimes highly concentrated in pore spaces. Minor hematite is also found replacing brachiopod shells. There are two zones of ferroan oolite and coated grains. Toward the top of the unit in two samples, nearly 80 percent of the detrital grains are coated by hematite mixed with what appears to be goethite and/or limonite. Close to the middle of the unit, another two samples show the same type of coatings although the amount of coated grains do not exceed 15 percent. These coatings give, in some instances, an oolitic appearance to the grains. Euhedral to subhedral iron-rich dolomite crystals are present in the upper half of the unit and range from 2.5 to 16 percent. Feldspar overgrowths are present throughout the unit; they range from 0.3 to 10.7 percent. Authigenic quartz is present along quartz grain boundaries; it ranges from 0.5 to 2.8 percent.

Matrix: The description for the matrix of the New Jersey Zinc B-1 drill hole (above), applies to the sandstones in this location. Matrix ranges from 0.3 to 14.3 percent.

Porosity: The average pore space found in this location is 14.5 percent.

Northern Natural Gas Vermillion 66-9 **(V66-9)**:

Texture and detrital mineralogy: The Mt. Simon Sandstone in this location is rather homogeneous both texturally and mineralogically. Most of the samples have a bimodal texture as described above on the New Jersey Zinc B-1 drill hole. Bioturbated thin silty beds are present towards the bottom of the unit. Detrital quartz comprises 72.7 percent (mostly common quartz with minor amounts of polycrystalline and vein ? quartz). Feldspar is present in all samples and ranges from 0.3 to 5 percent. Plutonic rock fragments are found in 16 of 22 samples, ranging from 0.2 to 1.7 percent. Brachiopod shells were found in only one sample in the uppermost part of the unit near the contact with the overlying Eau Clair Formation, and constitute 19 percent of the sample.

Authigenic mineralogy: Potassium feldspar is the most abundant authigenic mineral, ranging from 0.3 to 7 percent. Quartz, calcite, dolomite and pyrite are present in minor quantities (usually less than 4 percent).

Matrix: Matrix was only found toward the bottom of the unit near the contact with the Precambrian Solor Church Formation. The matrix consists of potassium-rich silts and clays, as evidenced by the yellow staining seen in thin section.

Porosity: The average pore space found in this location is 16 percent.

CLASSIFICATION:

Petrographic analysis of all the thin sections shows

two main rock types in the Mt. Simon Sandstone (See Table 1 and Figure 4). Sixty percent of the samples were classified as quartz sandstones (or, quartz arenites according to Pettijohn, Potter and Siever, 1987, p.145). These sandstones contain less than 5 percent of either feldspar or rock fragments (=lithics). The second most abundant rock type (39 percent of all samples), is feldspathic sandstone (subarkose according to Pettijohn, Potter and Siever, 1987, p.145). These sandstones contain between 5 and 25 percent detrital feldspar and generally have little or no rock fragments. Only two samples were classified as sublithic sandstones (or, sublitharenites according to Pettijohn, Potter and Siever, 1987, p.145). These rocks contain between 5 and 25 percent rock fragments (in this case between 5 and 7 percent), and little or no detrital feldspar.

An important parameter in the classification of rocks from the Mt. Simon Sandstone is the grain size distribution. Fine- to very fine-grained sandstones are usually feldspathic and medium- to coarse-grained sandstones usually contain very little or no detrital feldspar (quartz sandstones). Many times a combination of these two extremes is seen when the rocks present a bimodal distribution; in this case the coarser grains are mostly quartz and the finer fraction contains both quartz and feldspar grains (Plate 2-G).

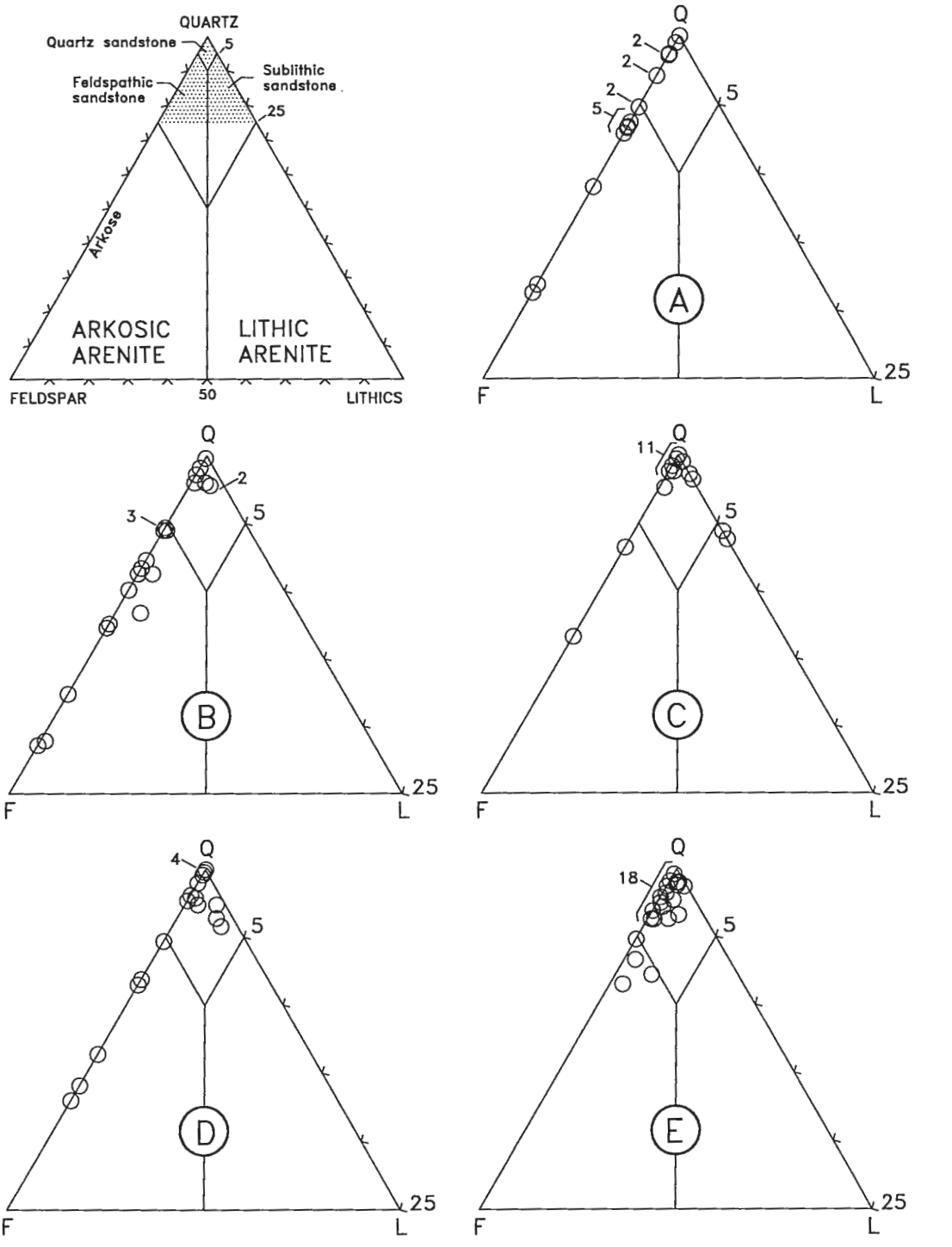

Fig. 4: Classification of the Mt. Simon Sandstone for each of the 5 drill holes. **(A)** Northern Natural Gas Hollandale 1-A (H1A); **(B)** New Jersey Zinc B-1; **(C)** Pan Ocean Oil, Ltd.SQ9; **(D)** Minnegasco KAN-1 and SCH-1; **(E)** Northern Natural Gas Vermillion 66-9. Sandstone classification (upper left) modified from Pettijohn, et al. (1987, p. 145).

CHAPTER IV

AUTHIGENIC FELDSPAR IN SANDSTONES

The principal objective of this chapter is to bring together some general observations about feldspar authigenesis in sandstones that will clarify the relationships between detrital and authigenic feldspars in the Late Cambrian Mt. Simon Sandstone. A fairly complete list of publications related to feldspar authigenesis is shown in Appendix 1, and this represents an important, up-to-date research tool for future studies in this field.

Hundreds of papers describing particular cases of feldspar authigenesis on different sandstone units have been written in the last five decades. However, few studies have covered the subject in a broad sense. One of the earliest of these studies was by Tester and Atwater (1934); they presented a literature review of studies done on secondary feldspars since 1861. By studying a large number of thin sections of rocks from Cambrian to Cretaceous in age, the authors demonstrated the abundance of authigenic feldspar as opposed to what had been said about authigenic feldspar being of rare or uncommon occurrence. Baskin (1956) reported the presence of authigenic feldspars in samples from forty localities. His study was primarily focused on the differences between authigenic and non-authigenic feldspars, and he proposed an epigenetic or replacement origin for most authigenic feldspars. Kastner and Siever (1979) studied the geochemical and geological conditions under which feldspars form at the relative low temperatures and pressures characteristic of unmetamorphosed sedimentary rocks. They estimated that approximately five percent of all feldspars in continental sedimentary rocks are

authigenic alkali feldspars, based on a complete literature review and their own observations of several hundred thin sections of limestones, sandstones and shales.

POSSIBLE ORIGINS:

Several theories have been proposed for the formation of authigenic feldspar in sandstones. A common hypothesis in the late 1800s and early 1900s was based on syngenetic processes; feldspar were believed to grow on the sea floor during a period of slow sedimentation in the still unconsolidated mud (Tester and Atwater, 1934; Van Straaten, 1948). Tester and Atwater stated that the best evidence for growth during deposition is in the nature of the inclusions (carbonaceous matter, clay particles, calcite and dolomite fragments) often found in the feldspar. Another reason for this assumption was the belief of the impossibility of having crystals of idiomorphic habit growing in a lithified rock (Van Straaten, 1948). Baskin (1956, p. 152) stated: "Although final conclusions cannot be drawn regarding the origin of most authigenic feldspars, the available evidence points toward a replacement or epigenetic origin". He presented three important observations to explain the impossibility of a syngenetic origin for the feldspars and also stressed the importance of meteoric waters in the crystallization of authigenic feldspars within the sediments. It is clear that there has been some controversy between the idea of a syngenetic versus an epigenetic or authigenic origin for feldspar in sandstones. A classic example is represented by the paper written by Woodard (1972) and the discussion by Odom (1974). Woodard demonstrated a syngenetic origin for sanidine beds from the Middle Ordovician Saint Peter Sandstone in Wisconsin; Odom indicated that the feldspar, which should not be called

sanidine, was formed epigenetically as overgrowths on detrital K-feldspar grains at low temperatures.

Kastner and Siever (1979) presented perhaps the most complete geochemical model for authigenic feldspar formation. Their conclusions were based on an extensive study of authigenic feldspars, including petrography, geologic occurrence, chemical and physical characteristics, and low temperature thermodynamics. The authors introduced two geochemical models for feldspar formation, an isochemical model (closed system) and an exchange reservoir or mass transfer model. "The major difference between isochemical models and mass transfer or exchange reservoir models is the movement of fluids from one reservoir to another, involving substitution or mixing of two fluids of different composition." (Kastner and Siever, 1979, p. 471).

The authigenic origin of feldspar in sandstones has also been described by a number of authors in the last decade. The advantages of the progress of science in the last ten years has lead to the dating of authigenic feldspars, which is a complicated task and an important tool to determine the age of the diagenesis in a sedimentary unit. One of the most recent studies of dates and origins for potassic diagenesis was done by Duffin (1990). In his Ph.D. thesis, Duffin reported potassic diagenesis of Cambrian-Ordovician sandstones and Precambrian basement rocks of the North American Midcontinent.

Another old theory on feldspar formation was based on hydrothermal activity. The basis for this theory was the unsuccessful attempt to produce feldspars under normal conditions of pressure and temperature. Most authors defending this idea believed that there is a relationship

between the mineralization of Mississippi Valley type ore deposits and feldspar mineralization, both being a result of hydrothermal solutions related to the ore-bearing solutions (Goldich, 1934). Many writers, however, reject a metamorphic or hydrothermal origin due to the widespread occurrence of feldspars in time and place in rocks that have no evidence of metamorphic or hydrothermal action. Also, as stated by Baskin (1956), the term hydrothermal is vague and a distinction between igneous, metamorphic and volcanic processes and meteoric waters should be made. These waters are also at higher temperatures than the surface waters and are not only closely related to their sedimentary environment, but are an important factor in feldspar diagenesis (Baskin, 1956).

One more theory for the formation of authigenic feldspar has been proposed by Long and Lyons (1992) and Duffin et al. (1989). These studies emphasize the importance of acid systems in the formation of authigenic feldspar. Brines rich in potassium, with a high Eh and a low pH, developed in arid conditions such as those in southern Australia (Lake Tyrrell), play an important role in precipitation of authigenic potassium feldspar (Long and Lyons, 1992).

An important point in the discussion of the origin of authigenic feldspars is related to the source of solutions that provide the proper ions for feldspar precipitation. Meteoric waters from nearby environments moving through a porous media such as a sandstone can provide the necessary elements for feldspar formation. More distant sources for these solutions have been suggested, such as tectonically expelled fluids from orogenic belts (Aleinikoff, et al., 1993; Deming, 1992; Hearn et al., 1987; Hearn, 1985; Leach

and Rowan, 1986; Oliver, 1986). Other theories require no movement of solutions; in-situ framework grain dissolution can provide the necessary constituents for precipitation of feldspar and\or replacement of other minerals by feldspar.

Perhaps none of the theories on the formation of authigenic feldspar are unique for any particular case. It is most likely that a combination of some of the processes mentioned here are in the end responsible for the formation of authigenic feldspar not only in the Cambrian Mt. Simon Sandstone in southeastern Minnesota but also in different sandstone sequences throughout the world.

PETROGRAPHY:

Even though authigenic feldspars are normally a small fraction of the feldspars in a rock (Kastner and Siever, 1979), they are rather easy to identify under the polarizing microscope due to their idiomorphic crystalline shape. Overgrowths showing straight edges and sharp corners, usually of rhombohedral shape, are common around detrital feldspar grains in the Late Cambrian Mt. Simon Sandstone in southeastern Minnesota. In most cases the overgrowths are developed around detrital cores of microcline and orthoclase and usually are not in optical continuity with them. These relationships will be described in more detail in a separate chapter. Commonly detrital feldspar cores are not visible or are simply absent. There are two possible explanations for the lack of cores; either the feldspar grew without the existence of a nucleation center or it is just a section of the overgrowth oriented in such way that the core is not intersected by the thin section cut and therefore not visible. Kastner and Siever (1979) stated that almost all authigenic microclines and a high proportion of authigenic

K-feldspar grow around K-feldspar detrital cores.

Grain size is an important factor in the mineralogical classification of certain sandstone units. Odom (1975) studied more than 700 samples from Cambrian sandstones in the Upper Mississippi Valley; in his petrographic studies he determined that in most cases feldspar was concentrated in the <0.125 mm sand range. This is particularly true for the Cambrian Mt. Simon Sandstone where most of the detrital and authigenic feldspar are concentrated in the fine to very fine sand fractions.

GEOCHEMISTRY:

Studies on the chemistry of authigenic feldspar became an easier task in the 1970s with the use of microprobe analysis. Stablein and Dapples (1977) studied Cambrian sandstones in western Wisconsin; their studies involved electron microprobe analysis of cores and overgrowths of 197 K-feldspar grains throughout the Cambrian Tunnel City Group. They found the overgrowths to be pure orthoclase and the cores to have an average of 93 percent orthoclase in composition.

Without a doubt, the most complete study on the chemistry and thermodynamics of authigenic feldspars was done by Kastner and Siever (1979). Electron microprobe analysis performed by these authors showed that authigenic feldspars are pure albites and pure K-feldspars; their pureness makes them one of the best natural representatives of end members of the alkali feldspar series. This fact is confirmed on the Cambrian Mt. Simon Sandstone in the thesis area. According to Pettijohn et al. (1987, p. 461), the ideal chemical conditions for the formation of authigenic

feldspar are a high enough concentration of dissolved silica (from skeletal parts of organisms or from hydrolyzing silicates) and a high enough ratio of Na^+/H^+ or K^+/H^+ ions (from pore waters). The chemical reactions that form authigenic feldspar are shown in Table 2.

In some instances, detrital K-feldspar and calcic plagioclases in sandstones are replaced by albite during burial diagenesis. The replacement is either direct or in other cases there is a prior replacement of the K-feldspar by other minerals (anhydrite, calcite, and dolomite) before albitization occurs (Walker, 1984; Carozzi, 1993, p. 22). If not detected, the process of albitization of feldspars could lead to a misinterpretation of provenance (Carozzi, 1993, p.23). The reactions involved in this process are shown in Table 3.

METHODS:

The methods used in the study of authigenic feldspars are common for most diagenetic studies. The following descriptions are based on the importance and usefulness of each method.

The petrographic microscope:

This is one of the most important and inexpensive tools in diagenetic studies. It is the basis for understanding textural relationships between detrital and authigenic minerals (Burley et al., 1985). By point counting a thin section, the petrographer can determine the amounts and relationships between detrital and authigenic components and porosity. These parameters are important to determine what type of studies should be done next. Thin sections are

Table 2. Geochemical reactions forming authigenic feldspar in the subsystem SiO_2-Al_2O_3-K_2O-Na_2O-H_2O (After Pettijohn, et. al., 1987, p. 461 and Kastner and Siever, 1979, p. 459).

1. Kaolinite to Na- or K-feldspar:

   $Al_2Si_2O_5(OH)_4 + 2K^+ + 4(H_4SiO_4) \rightarrow 2KAlSi_3O_8 + 9H_2O + 2H^+$

   $Al_2Si_2O_5(OH)_4 + 2Na^+ + 4(H_4SiO_4) \rightarrow 2NaAlSi_3O_8 + 9H_2O + 2H^+$

2. Muscovite to K-feldspar:

   $KAl_2(AlSi_3)O_{10}(OH)_2 + 2K^+ + 6(H_4SiO_4) \rightarrow 3KAlSi_3O_8 + 12H_2O + 2H^+$

3. Na-Al Smectite to Na- or K-feldspar:

   $Na(Al_5Mg)Si_{12}O_{30}(OH)_6 + 4Na^+ + 3(H_4SiO_4) \rightarrow 5NaAlSi_3O_8 + 8H_2O + 2H^+ + Mg^{++}$

   $Na(Al_5Mg)Si_{12}O_{30}(OH)_6 + 5K^+ + 3(H_4SiO_4) \rightarrow 5KAlSi_3O_8 + 8H_2O + 2H^+ + Na^+ + Mg^{++}$

4. Analcime to albite:

   $Na(AlSi_2O_6)\cdot H_2O + H_4SiO_4 \rightarrow NaAlSi_3O_8 + 3H_2O$

5. Analcime to K-feldspar:

   $Na(AlSi_2O_6)\cdot H_2O + H_4SiO_4 + K^+ \rightarrow KAlSi_3O_8 + Na^+ + 3H_2O$

6. Phillipsite to K-feldspar:

   $(\frac{1}{2}Ca,Na,K)_5(Al_5Si_{11}O_{32})\cdot 10H_2O + 2K^+ + 4(H_4SiO_4) \rightarrow 5KAlSi_3O_8 + \frac{5}{2}Ca^{++} + 5Na^+ + 18H_2O$

Table 3. Geochemical reactions involved in the albitization of K-feldspar (After Walker, 1984, p. 15).

Precursor replacements:

1. Replacement of potassium feldspar by anhydrite:

   $KAlSi_3O_8 + Ca^{++} + SO_4^{--} + 8H_2O \rightarrow CaSO_4 + 3H_4SiO_4^0 + Al(OH)_4^- + K^+$

2. Replacement of potassium feldspar by calcite:

   $KAlSi_3O_8 + Ca^{++} + HCO_3^- + 8H_2O \rightarrow CaCO_3 + 3H_4SiO_4^0 + Al(OH)_4^- + K^+ + H^+$

3. Replacement of potassium feldspar by dolomite:

   $KAlSi_3O_8 + Ca^{++} + Mg^{++} + 2HCO_3^- + 8H_2O \rightarrow CaMg(CO_3)_2 + 3H_4SiO_4^0 + Al(OH)_4^- + K^+ + 2H^+$

Albitization:

4. Direct replacement of potassium feldspar by albite:

   $KAlSi_3O_8 + Na^+ \rightarrow NaAlSi_3O_8 + K^+$

5. Replacement of anhydrite by albite:

   $CaSO_4 + 3H_4SiO_4^0 + Na^+ + Al(OH)_4^- \rightarrow NaAlSi_3O_8 + Ca^{++} + SO_4^{--} + 8H_2O$

6. Replacement of calcite by albite:

   $CaCO_3 + 3H_4SiO_4^0 + Na^+ + Al(OH)_4^- + H^+ \rightarrow NaAlSi_3O_8 + Ca^{++} + HCO_3^- + 8H_2O$

7. Replacement of dolomite by albite:

   $CaMg(CO_3)_2 + 3H_4SiO_4^0 + Na^+ + Al(OH)_4^- + 2H^+ \rightarrow NaAlSi_3O_8 + Ca^{++} + Mg^{++} + 2HCO_3^- + 8H_2O$

usually stained for distinguishing K-feldspar from plagioclase and quartz. The study of optical properties of the feldspar cores and overgrowths is often difficult and sometimes impossible due to grain size (usually <0.125 mm).

Scanning electron microscope (SEM):

The SEM has became a very valuable device in the study of micro-textures of authigenic minerals in sandstones (Bjørlykke, 1983). The most important features offered by the SEM are: an extreme depth of focus, a wide range of magnification (500 times greater than the petrographic microscope in some instances), and the importance of presenting a third dimensional view of the morphology of detrital and authigenic minerals. To provide a qualitative chemical identification of minerals, the SEM in some cases is equipped with a solid-state energy dispersive X-ray analyzer (EDS)(Burley, et al. 1985).

Electron microprobe:

As mentioned before, feldspar grains and particularly overgrowths are in many cases on the order of tenths to hundredths of a millimeter in diameter. The micro-probe uses an electron beam that can easily determine the chemical composition of fine-grained material. It is of great value when SEM/EDS analysis presents problems such as the take-off angle or 3-D geometry, overcoming absorption of X-rays (Burley, et al. 1985). Even though analytical work using the electron microprobe is complex and expensive, in many cases it provides the only credible method for collecting quantitative chemical data on extremely small grains and overgrowths (Scholle, 1981, p. 190).

Cathodoluminescence:

It provides information on the spatial distribution of trace elements in clastic grains and cements (Scholle, 1981). Low temperature authigenic feldspars are nonluminescent under electron bombardment in comparison with igneous and metamorphic grains (Kastner, 1971). This strong contrast makes this method an important tool for distinguishing authigenic feldspars from detrital cores.

Age determinations:

Dating of authigenic feldspars requires the mechanical removal and separation of overgrowths from detrital grains. This procedure is rather complicated and has been successfully accomplished in few cases. Hearn, et al. (1989) described air abrasion and settling techniques for the quantitative separation of authigenic overgrowths from mineral grains. The overgrowths are removed as micron-sized flakes by tangential collisions with the ceramic walls of an air-driven abrasion mill; then, the abraded material is separated and concentrated by suspension in water and collected in acetone-soluble filters (Hearn, et al., 1989). The most common radiometric techniques used in feldspar dating are: $^{40}K/^{40}Ar$, $^{40}Ar/^{39}Ar$ and $^{206}Pb/^{204}Pb$. Duffin (1990) reported a K/Ar date from authigenic K-feldspar (near the base of the Mt. Simon Sandstone of Illinois) of 394.6 ± 6 Ma (Early Devonian). He stated that similar potassic diagenesis of the Mt. Simon Sandstone in Illinois occurs on a regional scale in the Upper Midcontinent area. Hearn, et al. (1987) reported $^{40}Ar/^{39}Ar$ dates on overgrowths of detrital K-feldspars in Cambrian carbonate rocks from Pennsylvania, Maryland, Virginia, and Tennessee. These dates range from 278 to 322 Ma (Late Carboniferous - Early

Permian). Aleinikoff et al. (1993) described overgrowth separation and reported more studies on the timing of K-feldspar formation in the mid-continent and southern Appalachian regions.

CHAPTER V

HEAVY ACCESSORY MINERALS

Twenty representative samples from four of the five drill holes were selected for heavy mineral concentrations. The drill hole not chosen for sampling was the Hollandale H1-A, due to the limited amount of sample and also to the high amount of cement in most of the samples. Eleven heavy mineral mounts were quantitatively studied (See Table 4 and Figure 5). Some of the heavy mineral mounts were not grain-counted due to either the scarcity of grains or to the excessive concentration of opaques (mainly pyrite). High concentration of carbonates and diaspore in the Pan Ocean Oil SQ-9 drill hole (SQ-9) was also an obstacle in the quantitative mineralogical estimate of these sands. The samples chosen for analysis were evenly distributed throughout the unit; one near the top, one toward the middle and one near the base (at an average of 135 feet from each other). The only exception was in the SQ-9 drill hole where only two samples were analyzed, one toward the top of the unit and the other toward the middle to lower part of the unit (121 feet apart). See the introduction for the location of the drill holes.

The purpose of this heavy mineral study is to clarify some diagenetic processes in the Mt. Simon Sandstone and also to corroborate the mineralogical and textural maturity of the sands (multicycle origin ?) by means of their ZTRG index (see definition below), and the degree of roundness, among other characteristics.

Sample preparation: The following steps were followed to achieve a successful preparation of the samples:

SAMPLE #	ZIRCON					TOURMALINE											RUTILE				
	RND		SUBRND - SUBANG		TOTAL	RND					SUBRND - SUBANG					TOTAL	RND		SUBRND		TOTAL
	ZONED	UNZONED	ZONED	UNZONED		GREENISH BROWN	GREEN	BLUE	PINK	VIOLET	GREENISH BROWN	GREEN	BLUE	PINK	VIOLET		YELLOW	RED	YELLOW	RED	
RU-B1-419	15.7	11.3	7.3	12.7	47.0	6.0	2.3	0.3	0.7	0.3	6.7	0.3			0.7	17.3	0.7		0.3		1.0
RU-B1-523	1.3	15.0	3.3	5.0	24.7	6.0	0.7	0.3			4.3	1.3		0.7		13.3				0.3	0.3
RU-B1-695	15.3	11.0	24.7	15.3	66.3	6.3	1.0	1.0			16.7	2.7		0.7		28.3	1.7	0.7	1.0	1.0	4.3
RU-SQ9-545	8.7	5.3	36.0	20.3	70.3	1.0					3.0	0.7	0.3			5.0			2.3	0.7	3.0
RU-SQ9-666	11.7	16.7	30.0	27.3	85.7	1.3			0.3		3.3	0.7				5.7	0.7	0.3	2.3	0.3	3.7
RU-SCH-930	22.3	25.7	20.7	22.0	90.7	2.3	1.0		0.3		2.3	0.7		0.3		7.0		0.3	0.7		1.0
RU-KAN-1023	24.0	24.7	21.0	24.3	94.0	2.0	0.3				0.3	0.7		0.3		3.7	0.3	0.3		0.3	1.0
RU-KAN-1140	18.0	24.0	20.7	22.7	85.3	2.0		0.3			3.3	0.3	0.3			6.3	1.3	1.7	3.0	2.3	8.3
RU-669-675	16.3	13.0	15.7	11.0	56.0	6.0	2.3	0.3	1.0		8.7					18.3		0.3			0.3
RU-669-788	13.0	9.7	16.3	10.3	49.3	1.7		0.3			8.7	2.0		1.0		13.7	0.7				0.7
RU-669-885	31.3	26.7	7.3	5.0	70.3	13.0	0.7	0.3	0.7		9.3	0.7				24.7			0.3		0.3

SAMPLE #	GARNET						APATITE	AMPHIBOLE		PYROX.	EPIDOTE							
	RND		SUBRND - SUBANG		ANG	TOTAL	SUBANG	HORNBL. SERIES	TREM/ ACTIN	AUGITE/ DIOPS.	SUBANG	DIASP.	STAUR.	ANAT.	RX TYPE	Z+T+R+G	*	ZTRG INDX.
	COLOR-LESS	PINK BROWN	COLOR-LESS	PINK BROWN	COLOR-LESS		COLOR-LESS											
RU-B1-419	3.7	3.3	21.0	2.0	2.7	32.7	1.0							1.0	QTZSS	96.0	99.0	99.0
RU-B1-523	2.7	18.0	18.3	2.0		41.0	3.3	3.0	9.3	1.0	4.0				QTZSS	79.3	100.0	79.3
RU-B1-695							0.3		0.3					0.3	FLDSS	99.0	99.7	99.3
RU-SQ9-545							0.3					16.3		5.0	QTZSS	78.3	95.0	82.5
RU-SQ9-666							0.3					3.0		1.7	QTZSS	95.0	98.3	96.6
RU-SCH-930							0.7				0.7				QTZSS	98.7	100.0	98.7
RU-KAN-1023			0.7			0.7	0.7								FLDSS	99.3	100.0	99.3
RU-KAN-1140															QTZSS	100.0	100.0	100.0
RU-669-675	0.3	2.7	14.7	3.3		21.0	1.7		0.7		1.0			1.0	QTZSS	95.7	99.0	96.6
RU-669-788	0.3	0.3	27.7	1.3	2.0	31.7	1.0		0.3	0.7	2.3			0.3	QTZSS	95.3	99.7	95.7
RU-669-885							0.3						4.0	0.3	QTZSS	95.3	99.7	95.7

* = TRANSPARENT HEAVY MINERALS OMITTING MICAS AND AUTHIGENIC MINERALS (ANATASE)

Table 4: Petrographic summary of the heavy minerals in the Mt. Simon Sandstone.
- Values are calculated based on 300 grains per mount.
- Sample numbers give core name and footage in the core.

ABBREVIATIONS:

RND: Rounded
SUBRND-SUBANG: Subrounded to subangular
ANG: Angular
FLDSS: Feldspathic sandstone
QTZSS: Quartz sandstone
ZTRG: Zircon-Tourmaline-Rutile-Garnet index

HORNBL: Hornblende
TREM/ACTIN: Tremolite actinolite
PYROX: Pyroxene
DIOPS: Diopside
DIASP: Diaspore
ANAT: Anatase

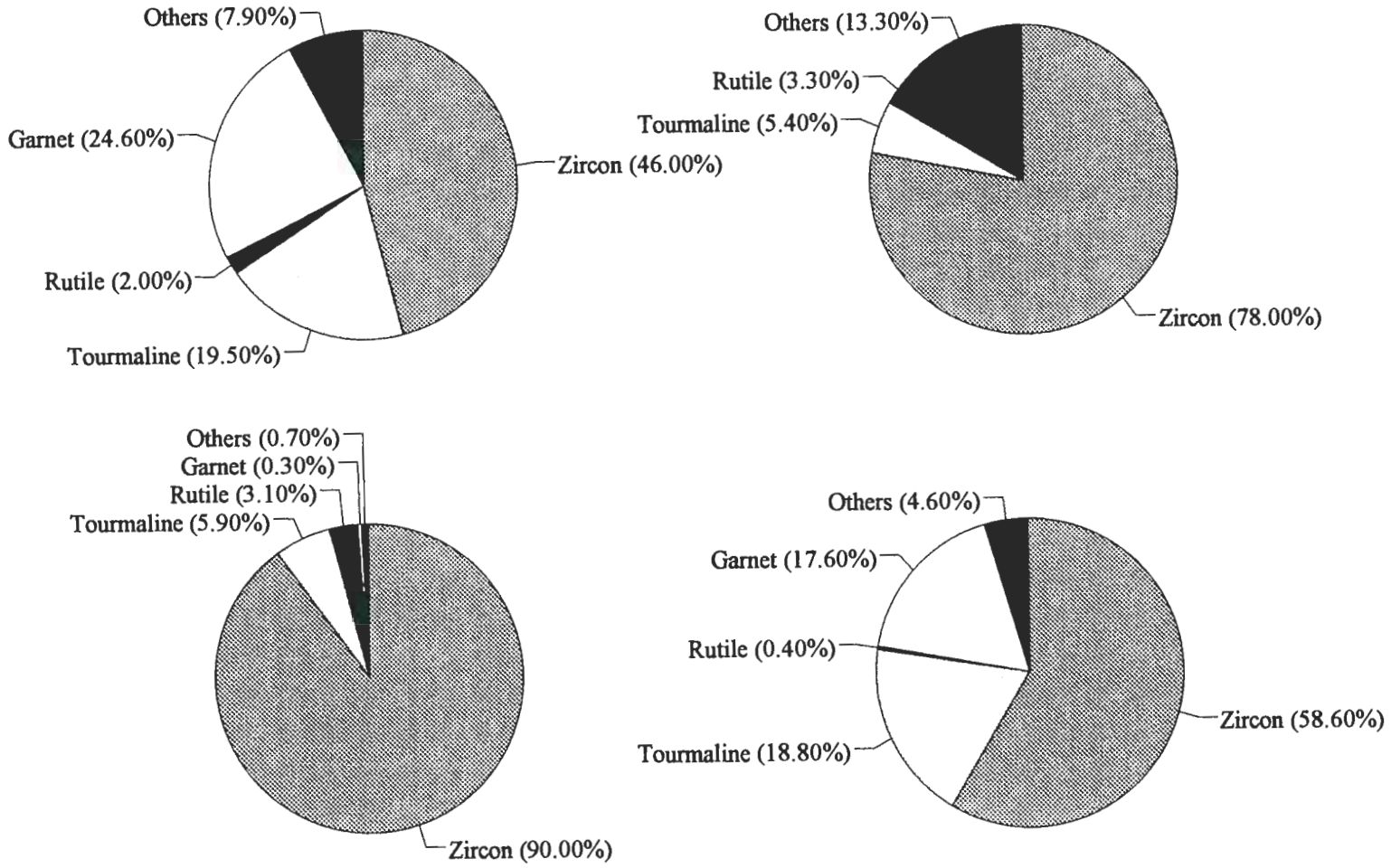

Fig. 5: Average heavy mineral composition of the four studied drill cores of the Mt. Simon Sandstone.

1. Disaggregation of the sandstone to liberate individual grains using a ceramic mortar and pestle.

2. Sieving of the loose material to eliminate the coarse fraction using a U.S. standard sieve mesh number 35 (0.5 mm.) on an ultrasonic sifter.

3. Analysis of the coarse fraction under the binocular microscope to verify the lack of heavy minerals.

4. Washing of the sample by repeated agitation using distilled water to eliminate clay particles and loose iron oxides.

5. Gravity separation of heavy minerals in separatory funnels using sodium polytungstate, a highly recommended, non-toxic, water-based heavy liquid with a density of 2.8 g/cm^2. The samples were stirred periodically in order to assure a good separation.

6. Cleaning of the heavy residue with distilled water and subsequent drying. The washings were collected for future recycling of the heavy liquid.

7. Separation of the highly magnetic fraction with a hand magnet.

8. When needed, separation of pyrite and other weakly or practically nonmagnetic opaques from the heavy fraction using the Frantz isodynamic magnetic separator. This task was not always successful.

9. The heavy mineral residue was split into two or four

portions when a considerable number of grains were present. The final portion was mounted in Canada balsam (n = 1.54) for petrographic analysis.

Counting procedure: All of the heavy mineral mounts were analyzed under a Zeiss polarizing microscope. A total of 11 grain mounts were chosen for grain counts. A total of 300 non-opaque grains per slide were identified and counted along randomly selected traverses (as many as needed depending on the amount of grains). All the grains within the field of view on each particular traverse were counted and plotted on a spreadsheet to calculate individual mineral percentages. The results are shown on Table 2.

MINERAL DESCRIPTIONS:

The percentages given here are based on the total average of non-opaque heavy mineral grains (including anatase) in the 11 mounts counted.

Non Opaques:

ZIRCON: Zircon is the most abundant non-opaque heavy mineral in the Mt. Simon Sandstone (average = 68.1 percent). The grains were counted within two main categories, rounded grains and subrounded to subangular grains. Each of these categories was subdivided according to the presence or absence of zonation in the grains. (Plates 3-A, 3-B, 3-C, 3-D & 3-E). The ratio of zoned to unzoned zircon grains as well as the ratio of rounded to subrounded/subangular zircon grains in the unit is almost one to one. Inclusions were observed in some of the grains. With few exceptions, most of the grains are elongated with an average length of 0.1 to 0.2 mm. The majority of the grains are colorless to

pinkish, and some have a reddish-yellow stain of iron oxide.

TOURMALINE: Tourmaline is the second most abundant non-opaque heavy mineral in the unit (average = 12.4 percent). Two factors were taken into account in the classification of tourmaline grains: a) The degree of roundness on the grains (rounded vs. subrounded/subangular), and b) the color (Plates 3-C & 3-D). The ratio of rounded to subrounded/subangular grains is close to 1:1 showing slightly more of the subrounded type. Most of the grains are ellipsoidal to spherical showing a grain size ranging between 0.15 and 0.3 mm. Nearly 80 percent of the grains are greenish to yellow-brown displaying a strong and distinctive pleochroism; the other 20 percent are varieties of green, blue, pink and violet color. Several grains showed inclusions.

RUTILE: Rutile is present in all samples ranging from 0.3 - 8.3 percent (average = 2.3 percent). Like tourmaline, rutile was classified according to the degree of roundness (rounded vs. subrounded) and color (Plates 3-A & 3-E). The ratio of rounded to subrounded grains is 2:1. The two color varieties observed are yellow-brown (amber) and red ("foxy red"). The ratio of yellow to red grains is also 2:1. Grain size ranges between 0.1 and 0.2 mm.

GARNET: Garnet was found in three drill holes, always toward the upper half of the unit. It ranges from 0.7 - 41 percent (average = 10.6 percent). Garnet grains were classified according to roundness (rounded, subrounded/subangular and angular) and color (colorless and pinkish-brown). Approximately 72 percent of the grains are subrounded to subangular, 24 percent are rounded and only 4 percent are angular. Most of the grains (75 percent) are

colorless. Grain size ranges from 0.1 to 0.3 mm. Dissolution features such as surface pitting and well-formed etch-facets are common in almost all grains (Plate 3-F).

APATITE: Apatite was found in small amounts ranging from 0.3 to 3.3 percent. All grains are subangular and colorless. Ragged edges are present on some of the grains due to dissolution processes.

AMPHIBOLE: Two types of amphiboles are present: hornblende and tremolite/actinolite.

Hornblende: Found only in one sample (RU-B1-523) from the easternmost drill hole (New Jersey Zinc B-1). It was recognized by its characteristic brown to bluish green color and pleochroism.

Tremolite/actinolite: Found in trace amounts except for the same drill hole mentioned above. It was recognized by the lack of color or in some instances very pale green color, ragged edges, inclined extintion and moderate birefringence.

PYROXENE (Augite/diopside): Trace amounts were found in only two samples (highest figure reached one percent). It was identified by its inclined extinction of 30° - 40° and its moderate birefringence.

EPIDOTE: Epidote was found in small amounts ranging from 2.3 - 4 percent. Most grains are subangular and very few rounded to subrounded. Epidote is part of the very fine-grained fraction and was identified mainly by its high relief and its irregular morphology.

DIASPORE: Diaspore is a ubiquitous nonopaque heavy mineral (density = 3.3 - 3.5 g/cm^3) in the westernmost drill hole (Pan Ocean Oil, Ltd. SQ-9). In this location, the Mt. Simon Sandstone directly overlies the Sioux quartzite in which diaspore is a common authigenic mineral. Only two heavy mineral mounts containing a small amount of diaspore were counted. Diaspore grains are colorless and usually show ragged edges indicating very little transport and/or dissolution processes (Plate 3-G). Grain size ranges from 0.1 to 0.3 mm. Diagnostic features for these grains are: high birefringence, parallel extinction and the presence of thin plates which reflect its structure.

STAUROLITE: Staurolite was only found in one sample (RU-669-885) toward the base of the Mt. Simon, in the Northern Natural Gas Vermillion 66-9 drill hole. In this location, staurolite makes up 4 percent of the total nonopaque heavy minerals. Grains are subangular to angular and grain size ranges from 0.1 to 0.2 mm. Other distinctive features used to identify this mineral were marked pleochroism (colorless to pale and golden yellow), high relief and quartz inclusions.

ANATASE: Authigenic anatase is present in almost all samples, ranging from 0.3 - 5 percent. Shades of blue and yellow are common together with a distinctive rectangular shape, in some instances showing an intergrowth of 2 or more crystals (Plate 3-H).

Opaques:

No count was made of the relative abundance of opaque heavy minerals in the Mt. Simon Sandstone. Pyrite, magnetite and hematite are the most abundant opaque heavy

PLATE 3

A: Sample RU-SQ9-652. Photomicrograph of zircon and rutile (R) grains in grain mount. Plain light, 0.8 mm across.

B: Sample RU-KAN-1140. Photomicrograph of single zircon grain (Zn). Note subangular to angular crystal faces, and zonation marked by the dashed lines. Plain light, 0.2 mm across.

C: Sample RU-KAN-1140. Photomicrograph of tourmaline (T) and zircon grains in grain mount. Tourmaline grains show lower relief compared to the surrounding zircon grains. Plain light, 0.8 mm across.

D: Sample RU-669-885. Photomicrograph showing detail of a tourmaline grain (T) and a zircon grain (Zn). Note inclusions in both grains. Plain light, 0.4 mm across.

E: Sample RU-KAN-1023. Photomicrograph showing rutile grain (R). Note "knee-shaped" twin and striations which are common features in rutile grains. The remaining grains in the field of view are zircons. Plain light, 0.4 mm across.

F: Sample RU-669-675. Photomicrograph of a single garnet grain (G). Note that chemical etching has produced a pitted surface on the grain. Plain light, 0.8 mm across.

G: Sample RU-SQ9-652. Photomicrograph of diaspore grains (D). Angular and ragged edges are due to a small amount of transport and dissolution processes. Note subangular tourmaline grain (T). Plain light, 0.8 mm across.

H: Sample RU-SQ9-666. Photomicrograph of authigenic anatase grain (An) and subrounded zircon (Zn). Authigenic anatase crystals are superimposed forming a composite grain. Plain light, 0.4 mm across.

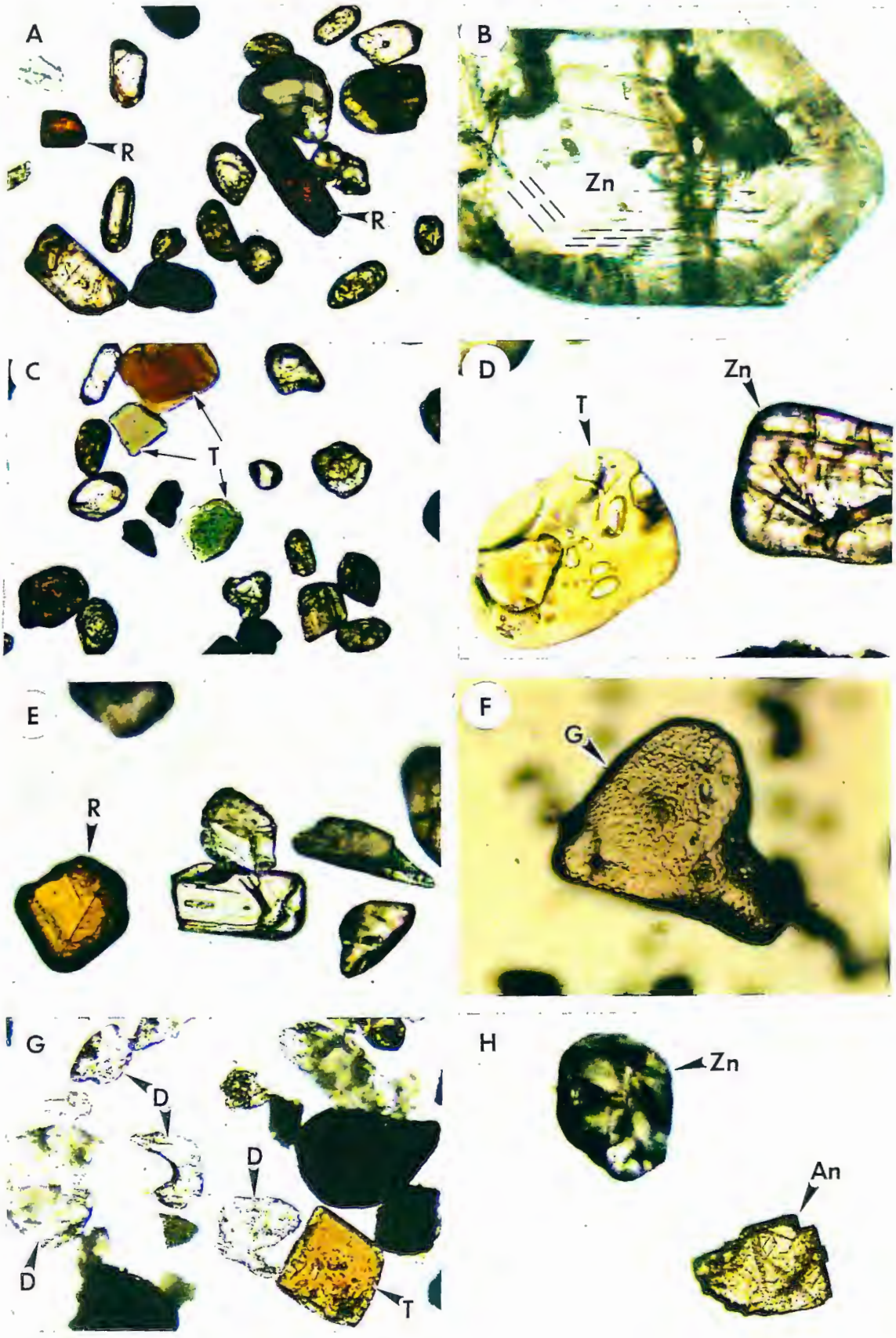
A
R
R
B
Zn
C
T
D
T
Zn
E
R
F
G
G
D
D
D
T
H
Zn
An

minerals in the unit. Pyrite is usually present as well developed euhedral crystals (authigenic). Detrital pyrite grains are present in minor quantities. Subrounded to rounded, fine- to medium-grained magnetite (present in most of the samples) was separated with a hand magnet before grain mounting. Hematite, both detrital and authigenic, was separated using the Frantz isodynamic magnetic separator.

MINERALOGICAL MATURITY:

Mineralogical maturity in a sandstone has been satisfactorily determined according to the ratio of quartz + chert to feldspar + rock fragments. In addition to this approach, Hubert (1962) proposed a zircon - tourmaline - rutile maturity index for sandstones (ZTR index), defined as the combined percentage of zircon, tourmaline and rutile among the transparent heavy minerals omitting micas and authigenic minerals. Detrital heavy mineral assemblages of sandstones are in most cases a function of the proportions of the different heavy minerals eroded from the source area, and the degree of modification of the detritus by abrasion and selective sorting during transportation and deposition (Hubert, 1962).

The ZTR index was calculated for each one of the eleven samples grain-counted in the Mt. Simon. Four of the eleven samples, classified as quartz sandstones (highly mature sandstones), showed a rather low ZTR index (below 75 percent). This anomaly was due to a rather high concentration of garnet (ranging from 21 to 41 percent) in the samples. Garnet is fairly resistant to abrasion and chemical attack, and therefore was considered in this study as part of the chemically and mechanically stable minerals on Hubert's original ZTR index. Consequently, a ZTRG index

is proposed in this study, as the percentage of zircon, tourmaline, rutile and garnet among the non-opaque, non-micaceous detrital heavy mineral fraction in a sandstone.

After calculating the ZTRG index for all samples (Table 2), 9 of the samples show indices above 95.7 percent, which indicates a high mineralogical maturity. This coincides with the mineralogical maturity of the sandstones as indicated by the high ratios of quartz to feldspar and rock fragments.

CHAPTER VI

DIAGENESIS

The concept of diagenesis was first properly described by J. Walther a century ago (1893 - 1894), as cited by Dunoyer de Segonzac (1968). He defined it as follows:

> "By diagenesis we mean all the physical and chemical changes that a rock undergoes from the time of its deposition, other than changes due to the intervention of tectonic compression and volcanic heat."

This idea has not changed at all through time. Pettijohn et al. (1987) described diagenesis as follows:

> "We use the term diagenesis to include all those processes, chemical and physical, which affect the sediment after deposition and up to the lowest grade of metamorphism, the green-schist facies."

The purpose of this chapter is to describe petrographic observations, integrated with some chemical data, to place important constraints on the nature and relative timing (paragenesis) of authigenic mineralization in the Mt. Simon Sandstone. In addition, dissolution processes (secondary porosity) in the unit are described.

Refer to Table 1 and drill core descriptions shown in the previous petrography chapter for the average percent of authigenic minerals in the unit.

AUTHIGENIC MINERALOGY:

Quartz: Quartz cement in the unit is not present as euhedral overgrowths. Instead, quartz cement is present at

contacts or boundaries between detrital quartz grains as part of an incipient pressure solution stage (Plate 4-A). This is evidenced in some samples in which very small amounts of other cements are present in rather durable hand specimens. Quartz overgrowths present in the samples from the Pan Ocean Oil, Ltd. SQ-9 drill hole were in some instances difficult to identify as either authigenic, or as part of locally derived quartz grains from the underlying Sioux Quartzite (i.e., recycled). The second possibility appeared to be more reasonable.

Feldspar: K-feldspar overgrowths occur on all detrital feldspars throughout the Mt. Simon Sandstone. Euhedral overgrowths show well-developed rhombic cross sections. In a few cases, anhedral overgrowths are present cementing detrital grains (Plate 4-B). Step-like facets or partially developed faces also occur (Plate 4-C). In the majority of the cases, the overgrowths are untwinned and not in optical continuity with the detrital cores (Plate 4-D). Rhombohedral feldspar crystals with the absence of detrital cores are present in some of the samples (Plate 4-E). As described before, this fact could mean that either the feldspar grew without the existence of a nucleation center, or it is just a section of an authigenic overgrowth oriented in such a way that the detrital core is not intersected by the thin section cut and therefore not visible.

Two samples were chosen for electron microprobe analysis. A total of five to six readings, including cores and overgrowths were done on each of nine grains (Plates 4-F, 4-G & 4-H). The results (Table 5) indicate that the overgrowths are essentially pure orthoclase ($KAlSi_3O_8$). Some authors have identified the authigenic feldspar of other rock units as sanidine (e.g., Marshall, et al., 1986;

PLATE 4

A: Sample RU-669-728. Photomicrograph showing quartz cement (Qc). Quartz cement is present along the boundaries between quartz grains (arrows). Plain light, 1.5 mm across.

B: Sample RU-669-867. Photomicrograph showing authigenic K-feldspar (Ov) on microcline grains (Mi; outlined by white dashed line). The anhedral overgrowth on the larger grain is cementing adjacent detrital quartz grains (Q). Crossed polarizers, 0.8 mm across.

C: Sample RU-669-867. Photomicrograph of K-feldspar overgrowth (Ov) on an altered detrital perthite (Pe?) grain. Note step-like facets on the overgrowth and adjacent quartz grains (Q). Crossed polarizers, 0.8 mm across.

D: Sample RU-H1A-1443. Photomicrograph of detrital orthoclase (Or) showing authigenic overgrowth (Ov). Note that the overgrowth is not in optical continuity with the detrital grain. Crossed polarizers, 0.2 mm across.

E: Sample RU-669-693. Photomicrograph showing authigenic K-feldspar (Af) and adjacent detrital quartz grain (Q). Note the absence of a detrital core. Crossed polarizers, 0.2 mm across.

F: Sample RU-H1A-1454. Photomicrograph of detrital orthoclase (Or) with authigenic overgrowth (rim = Ov). Points analyzed by electron microprobe are marked by dots. Crossed polarizers, 0.2 mm across.
1 (rim): $Or_{100}Ab_{0.0}An_{0.0}$; **2** (rim): $Or_{100}Ab_{0.0}An_{0.0}$; **3** (rim): $Or_{99.7}Ab_{0.0}An_{0.3}$; **4** (core): $Or_{91.5}Ab_{8.3}An_{0.1}$; **5** (core): $Or_{92.8}Ab_{6.7}An_{0.5}$.

G: Sample RU-H1A-1454. Photomicrograph of detrital orthoclase (Or) with authigenic overgrowth (rim = Ov). Points analyzed by electron microprobe are marked by dots. Crossed polarizers, 0.8 mm across.
1 (rim): $Or_{98.8}Ab_{1.1}An_{0.1}$; **2** (rim): $Or_{98.5}Ab_{1.3}An_{0.3}$; **3** (rim): $Or_{98.6}Ab_{1.4}An_{0.0}$; **4** (core): $Or_{91.9}Ab_{8.1}An_{0.0}$; **5** (core): $Or_{92.5}Ab_{7.1}An_{0.4}$; **6** (core): $Or_{91.4}Ab_{8.0}An_{0.6}$.

H: Sample RU-H1A-1454. Photomicrograph of detrital microcline and orthoclase with authigenic overgrowths (rims). Points analyzed by electron microprobe are marked by dots. Crossed polarizers, 0.8 mm across.
Grain 1 (G1): **1** (rim): $Or_{98.2}Ab_{1.4}An_{0.4}$; **2** (rim): $Or_{98.6}Ab_{1.1}An_{0.4}$; **3** (rim): $Or_{98.9}Ab_{0.4}An_{0.7}$; **4** (core): $Or_{95}Ab_{4.9}An_{0.1}$; **5** (core): $Or_{97.2}Ab_{2.6}An_{0.1}$; **6** (core): $Or_{96.1}Ab_{3.8}An_{0.1}$.
Grain 2 (G2): **1** (rim): $Or_{99.1}Ab_{0.5}An_{0.4}$; **2** (rim): $Or_{99.3}Ab_{0.1}An_{0.5}$; **3** (rim): $Or_{99}Ab_{0.9}An_{0.1}$; **4** (core): $Or_{96.4}Ab_{3.5}An_{0.1}$; **5** (core): $Or_{93.9}Ab_{6.1}An_{0.0}$.

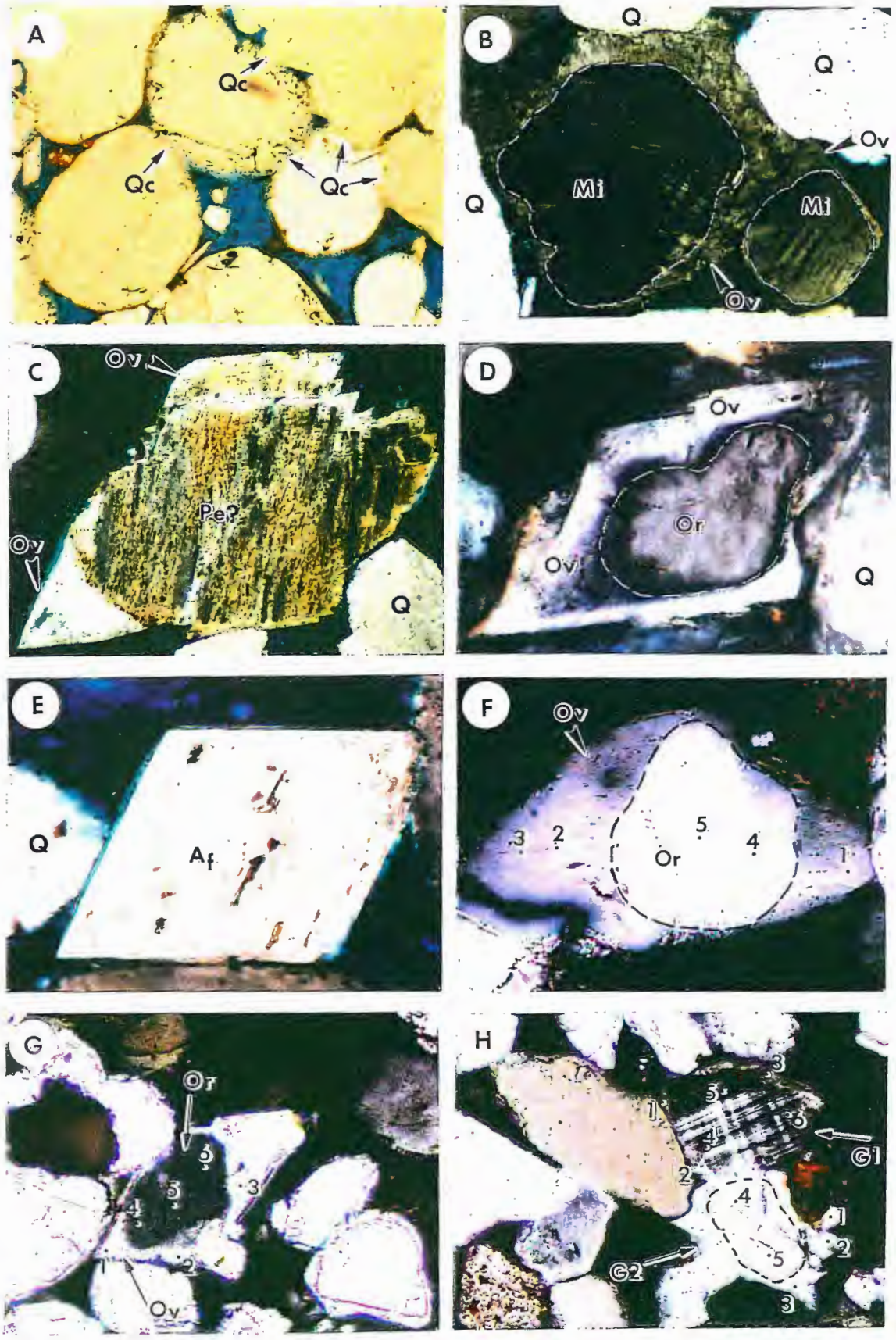
A
Qc
Qc
Qc
B
Q
Q
Ov
Mi
Q
Mi
Ov
C
Ov
Pe?
Ov
Q
D
Ov
Or
Ov
Q
E
Q
Af
F
Ov
3
2
1
5
Or
4
1
G
Or
5
4
5
3
1
2
Ov
H
3
5
1
4
5
2
G1
4
1
2
5
G2
3

	OVERGROWTHS	CORES
	%	%
SiO2	64.93	64.54
Al2O3	18.34	18.40
FeO	0.06	0.04
BaO	0.12	0.34
MgO	0.04	0.03
CaO	0.04	0.08
Na2O	0.06	0.63
K2O	16.63	16.19
Total	100.22	100.26
Number of ions on the basis of 24 oxygens.		
Si	9.00	8.96
Al	2.99	3.01
Fe 3+	0.00	0.00
Mg	0.01	0.00
Na	0.01	0.17
Ca	0.01	0.01
K	2.94	2.87
Ba	0.01	0.02
Total	14.97	15.04
Or	99.37	94.10
Ab	0.46	5.55
An	0.17	0.35

* NUMBER OF GRAINS = 9
* NUMBER OF POINTS PROBED PER OVERGROWTH = 2-3
* NUMBER OF POINTS PROBED PER CORE = 2-3

Table 5: Microprobe analysis of detrital and authigenic feldspars from the Cambrian Mt. Simon Sandstone. Average mole percentages of orthoclase (Or), albite (Ab) and anorthite (An) are also shown.

Odom, 1974; Woodard, 1972 and 1974). Standard mineralogy texts state that sanidine is a high temperature mineral restricted to volcanic rocks (e.g., Zoltai and Stout, 1984 p. 309). Furthermore, a single 2V determination (the only grain large enough and in the proper optical orientation) of 70° indicates a composition of orthoclase. Deer et al. (1992, p. 396) stated that 2V angles for low sanidine range from 0-54° and for high sanidine from 60-50°. Some other authors report even lower 2V angles for sanidine. The orthoclase molecule of the overgrowths averages 99.4 percent. Minor amounts (< 0.34 percent) of FeO, BaO, MgO and CaO were found in both cores and overgrowths. Due to the restricted number of polished thin sections available for microprobe analysis (n=4), only one grain was found with a considerable amount of albite molecule. This particular grain has a composition of $Or_{76.5}Ab_{23}An_{0.5}$; the overgrowth on this grain has a composition of $Or_{97.2}Ab_{2.0}An_{0.8}$. This overgrowth shows a slightly higher amount of albite than any of the other overgrowths present on microcline or orthoclase detrital grains. This could indicate that the chemical composition of the overgrowths is to a slight degree regulated by the chemical composition of the detrital core. All the other cores were either orthoclase or microcline (orthoclase molecule averages 94.1 percent) (Table 5). A discussion on the formation of the authigenic feldspar in the unit is presented in a previous chapter (Authigenic feldspar in sandstones).

Dolomite: Two types of authigenic dolomite were found in the unit: 1) Euhedral crystals with a distinctive rhombohedral habit, molded directly against the rounded edge of detrital quartz grains and authigenic feldspar in some cases, as described by Glover (1963, p. 40 in Pettijohn, etc. al, 1987, p. 449) (Plate 5-A). The long diagonals of

the rhombs range from 0.5 to 1 mm. Dolomite crystals can include significant percentages of ferrous iron in their crystal structure as a substitute for magnesium (Blatt, 1992, p. 288). This fact is true for these dolomite crystals, where two distinctive zones were observed; an iron-rich (red) core and an iron-poor or magnesium-rich (clear) outer rim. 2) Also as rhombohedral crystals although in this case not showing any evidence of zoning and also in smaller sizes (> 0.1 mm) (Plate 5-B). This type of dolomite was found replacing what appears to be stained illitic matrix. Dolomite replacing illitic layers was reported by Heald and Baker (1979) in the Mt. Simon and Rose Run Sandstones (Cambrian - Ordovician) of West Virginia and southern Ohio. The authors proposed iron- and magnesium-rich illite as the source of the ions in the dolomite.

Calcite: Authigenic calcite, as described by Pettijohn, et al. (1987, p. 46) is anhedral, made up of an interlocking crystal mosaic in which each crystal may vary from a few microns up to a centimeter (Plate 5-C). This texture is termed by different authors as "poikilotopic" cementation. The mosaic encloses detrital grains and authigenic minerals, including quartz, feldspar (cores and overgrowths), kaolinite cement, and probably other detrital and authigenic minerals that are beyond recognition due to complete replacement. Calcite is also present filling pore spaces.

Siderite (?): Siderite cement is only present in one sample (quartz sandstone). It is present as small crystals (> 0.1 mm) around quartz grains (Plate 5-D). Due to the extreme resemblance of this mineral to dolomite, definite conclusions cannot be made in regard to the classification of this authigenic mineral as siderite.

Kaolinite: Two types of kaolinite were seen in the sandstones: 1) As described by Carozzi (1993, p. 65), authigenic kaolinite is present as pore-filling packets or small stacks of plates ("kaolinite books"), randomly arranged with respect to each other (Plate 5-E). These vermicular aggregates are also present cementing detrital grains. 2) As a cryptocrystalline "groundmass" showing a laminae-like structure parallel to bedding. Authigenic kaolinite is recognized by many authors as derived from the diagenetic dissolution of detrital feldspar. This assertion may be applied to the Mt. Simon Sandstone due to the presence of feldspar dissolution in the unit.

Illite: Present in very few samples and in small amounts as partially dissolved thin (>0.1 mm) coatings on detrital grains (Plate 5-F). It displays a distinctive undulose extinction under crossed polars.

Pyrite: Authigenic pyrite is probably the latest cement in the Mt. Simon. It was found in most samples from two drill holes and is completely absent in the other three. It is present as euhedral and subhedral crystals filling pore spaces and replacing authigenic and detrital minerals (Plate 5-G) including the original material that makes up the brachiopod shales in the unit (collophane).

Hematite: Authigenic hematite was found (by coincidence ?) in the drill holes in which pyrite is not present (except for one of the drill holes in which neither pyrite or hematite are present). It is found usually as very small (few microns) specks around detrital grains (Plate 5-H). These micron-sized particles are concentrated in some areas, forming pore-filling patches of hematite cement. Hematite/limonite is found in a few samples as

PLATE 5

A: Sample RU-H1A-1522. Photomicrograph showing authigenic rhombohedral dolomite. Note iron-rich core (Dc) and iron-poor rim (Dr). Adjacent grains are detrital quartz grains (Q). Crossed polarizers, 0.8 mm across.

B: Sample RU-SQ9-575. Photomicrograph of authigenic dolomite (D) replacing illitic matrix (ILL; yellow). Note rhombohedral shape of the dolomite crystals (arrows). Plain light, 0.4 mm across.

C: Sample RU-SQ9-483. Photomicrograph showing poikilotopic calcite cement (c). Detrital quartz grains (Q) and kaolinite cement (K) are being replaced by calcite. Crossed polarizers, 1.5 mm across.

D: Sample RU-SQ9-630. Photomicrograph of detrital quartz grains (Q) partially cemented by finely crystalline siderite ? (S). Plain light, 1.5 mm across.

E: Sample RU-SQ9-474. Photomicrograph showing authigenic kaolinite (K). Larger vermicular stacks or "books" are present in the lower right corner. Crossed polarizers, 0.8 mm across.

F: Sample RU-669-728. Photomicrograph showing authigenic illite (I). The illitic cement is partially dissolved showing a thin coating around detrital quartz grains (Q). Plain light, 1.5 mm across.

G: Sample RU-SQ9-575. Photomicrograph showing authigenic pyrite (Py). Pyrite is filling pore spaces (shown blue) and replacing glauconite (g), feldspar (f)(grains and overgrowths) and detrital quartz grains (q). Plain light, 0.8 mm across.

H: Sample RU-H1A-1510. Photomicrograph showing authigenic hematite (H). Hematite in this case is cementing detrital quartz grains. Plain light, 0.8 mm across.

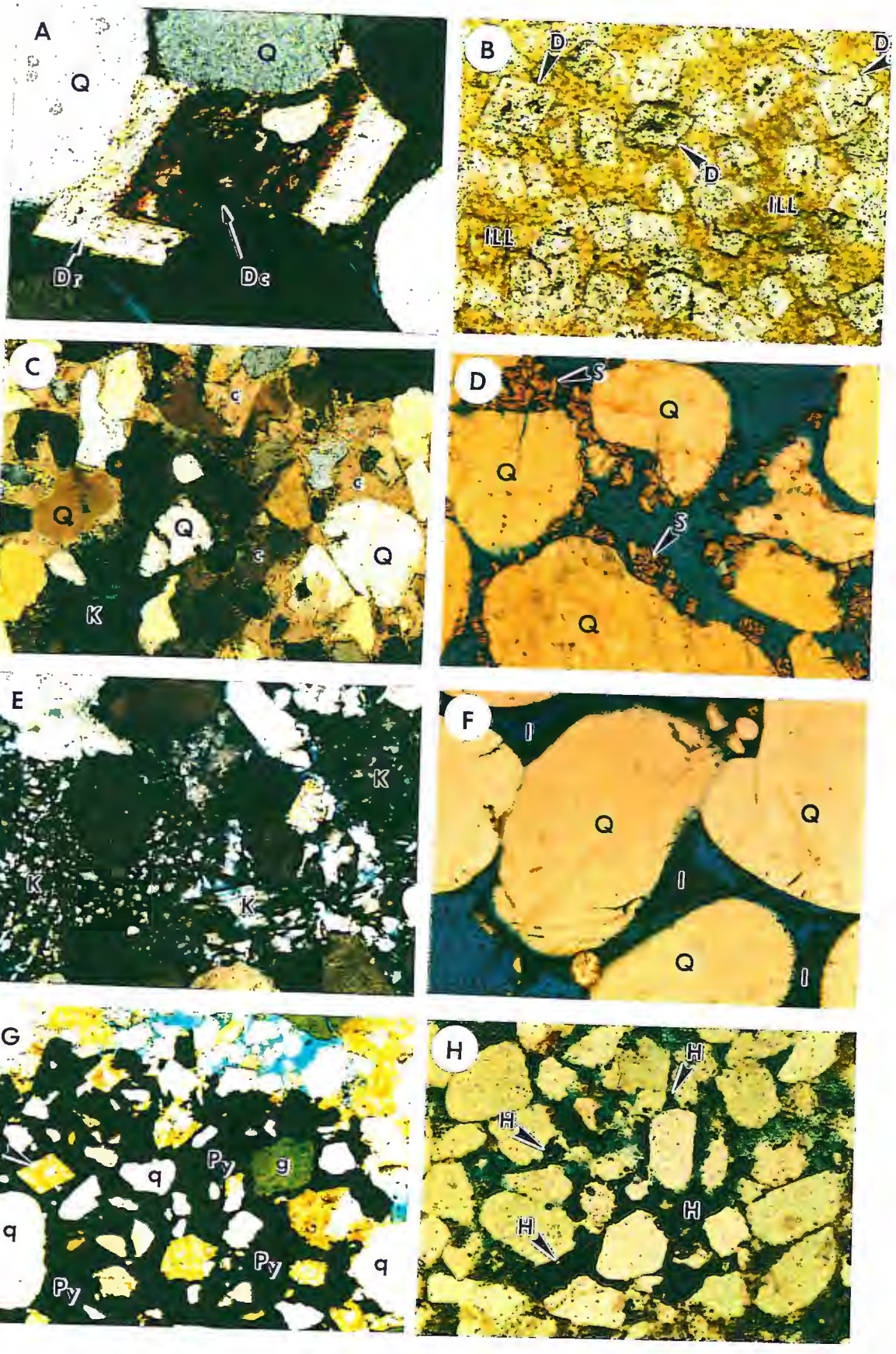
A
Q
Q
Dr
Dc
B
D
D
D
ILL
ILL
C
c
c
c
Q
Q
Q
K
D
S
Q
Q
S
Q
E
K
K
K
F
I
Q
Q
I
Q
I
G
q
Py
g
q
Py
Py
q
H
H
H
H
H

coatings on detrital grains.

Leucoxene: Minor quantities of this titanium oxide were found in the Northern Natural Gas Hollandale 1-A (H1A) drill hole. It is present as thin coatings around detrital grains. It is the only authigenic mineral found between detrital feldspars and their overgrowths (Plate 6-A).

PARAGENESIS:

The relationships among the different authigenic minerals in the unit were interpreted from the petrographic study of thin sections. Relative ages are given in this study for the paragenesis of authigenic minerals. These minerals were grouped in three main stages: 1) An early diagenesis stage represented by precipitation of leucoxene (titanium oxide), and iron oxides (hematite and limonite/goethite), 2) A burial diagenesis stage marked by the precipitation of quartz, potassium feldspar, kaolinite, illite (?), dolomite and siderite (?), and finally 3) A late diagenesis stage showing calcite and pyrite replacing most of the previous cements and filling pore spaces.

Although there is no evidence of dissolution of calcite cements in the unit, it is possible that this mineral was completely removed during burial diagenesis, prior to a second stage of cementation (late diagenesis). This assumption could be made since many ancient sandstones have undergone extensive carbonate cementation and subsequent dissolution.

DISSOLUTION:

A number of samples show evidence of dissolution

porosity in thin section. Petrographic evidence for the presence of secondary pores in the Mt. Simon include oversized pores, intragranular pores, and partially dissolved cements and matrix (Plates 6-B through 6-F). These and other types of secondary porosity have been described in detail by Schmidt and McDonald (1979). According to these authors, leaching of labile constituents (mostly feldspars and rock fragments) creates a large percentage of secondary sandstone porosity in many reservoir sandstones. Another very important mechanism that has been proposed for the formation of secondary porosity in ancient sandstones (Schmidt and McDonald, 1979) is the mesogenetic leaching of the carbonate minerals calcite, dolomite and siderite, caused by the decarboxilation of organic matter in strata adjacent to the sandstones during the course of organic maturation. Heald and Larese (1973), described partially dissolved feldspars in the Mississippian Berea Sandstone of West Virginia, and the Cambrian Mt. Simon Sandstone of Ohio. Minerals that show evidence of dissolution in the Mt. Simon in southeastern Minnesota include detrital and authigenic feldspars, dolomite, glauconite, and illite (?) (Plates 6-B, 6-C & 6-D). Some detrital grains are almost completely dissolved and are beyond recognition (Plate 6-E).

Even though estimates of the amount of primary vs. secondary porosity of the unit were not calculated, it is evident that dissolution processes are an important factor in the porosity of the sandstone.

PLATE 6

A: Sample RU-H1A-1617. Photomicrograph showing detrital orthoclase grains (Or) and overgrowths (Ov), and detrital quartz grains (Q). Note a coating of leucoxene (L) around detrital grains. The photo was taken with transmitted and reflected light. Crossed polarizers, 0.4 mm across.

B: Sample RU-H1A-1443. Photomicrograph of a partially dissolved detrital feldspar. The feldspar overgrowth (Ov) is probably more resistant to dissolution. The blue color in the photograph is showing pore space (Po). Adjacent detrital grains are quartz (Q). Plain light, 0.2 mm across.

C: Sample RU-B1-718. Photomicrograph of a partially dissolved dolomite crystal (D). Note dissolution patterns along preferred crystallographic directions within the mineral. Dark blue color in the photograph is showing pore space (Po). Adjacent grains are quartz grains. Crossed polarizers, 0.4 mm across.

D: Sample RU-SQ9-575. Photomicrograph of a partially dissolved glauconite pellet (G). Porosity (Po) is shown in blue. Plain light, 0.8 mm across.

E: Sample RU-669-856. Photomicrograph of an almost completely dissolved grain (center). Dissolution processes as shown here create secondary porosity in the sandstone. Plain light, 0.8 mm across.

F: Sample RU-669-856. Photomicrograph of oversized pore (Po) due to the dissolution of matrix (M) in the sandstone. Note also (lower left) a partially disolved dolomite (D) crystal. Plain light, 0.8 mm across.

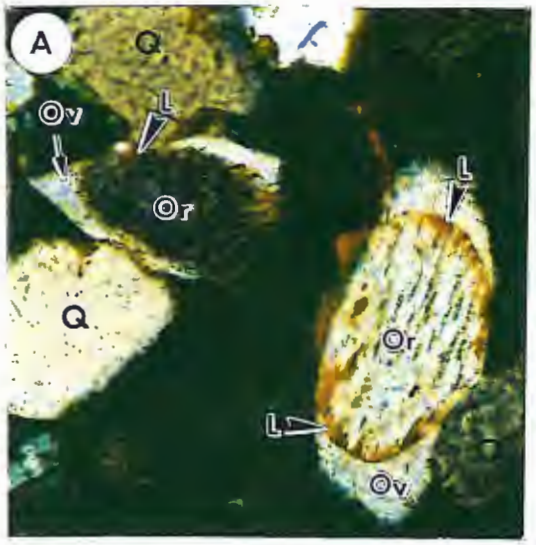
A
Q
Ov
L
Or
L
Q
Or
L
Ov

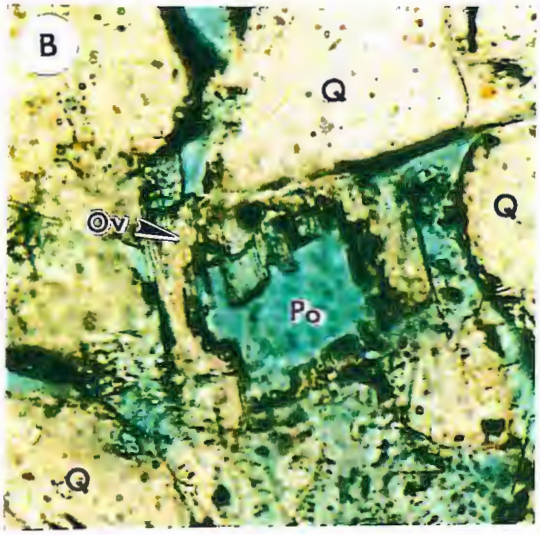
B
Q
Q
Ov
Po
Q

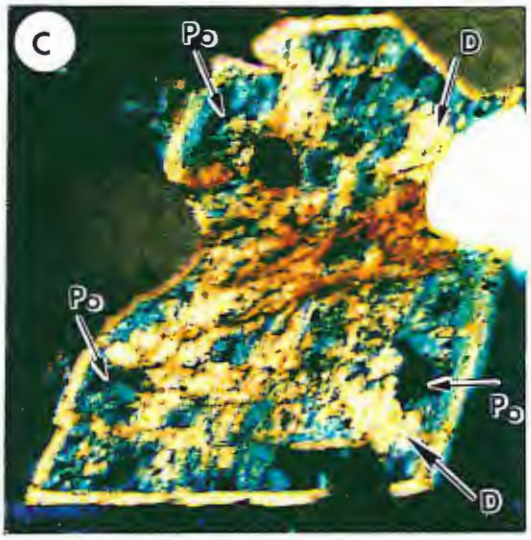
C
Po
D
Po
Po
D

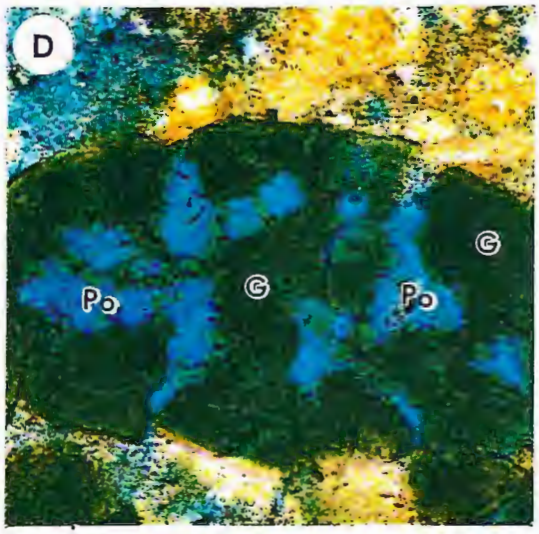
D
G
Po
G
Po

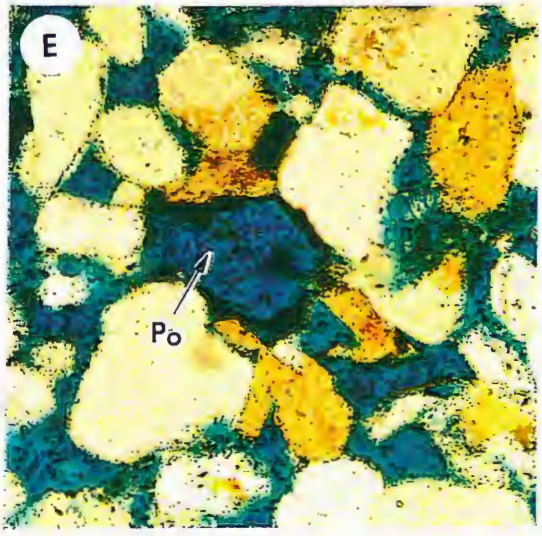
E
Po

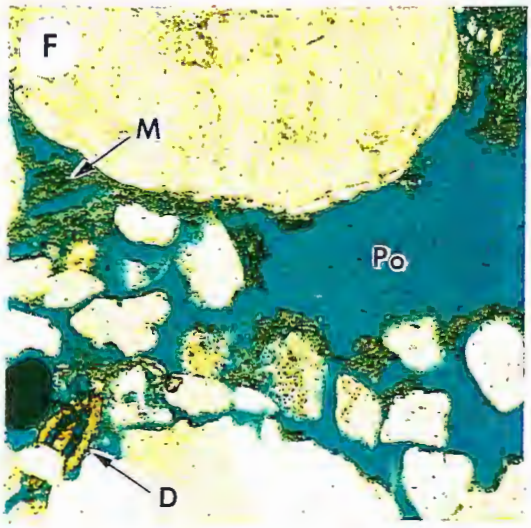
F
M
Po
D

CHAPTER VII

CONCLUSIONS

Data accumulated in this investigation support the following conclusions:

1) Petrographic analyses show that the Cambrian Mt. Simon Sandstone of southeastern Minnesota is mainly composed of quartz sandstones and feldspathic sandstones. The average composition, based on a total of 95 samples from five drill holes, is $Q_{95.4}F_{4.1}L_{0.5.}$. Other minor detrital components include rock fragments (igneous plutonic, intraformational siltstone and quartzite), micas (muscovite and biotite), glauconite, and brachiopod shells.

2) There is a direct relationship between detrital feldspar abundance and grain size. As observed by Odom (1975) and Odom et al. (1976), the feldspar is predominantly concentrated in the <0.125 mm sand size. In these samples, the feldspar percentage is as high as 21.4 percent.

3) Studies on the environments of deposition of the Mt. Simon Sandstone were not among the objectives of this study. Nonetheless, a marked bimodal texture found in several samples throughout the unit may be important evidence that suggests an eolian environment of deposition, perhaps in addition to the shore or nearshore environments suggested by Mossler (1992). The link between bimodality and eolian environments has been documented by Blatt (1992, p. 67) and Carozzi (1993, p. 7). As with any other sandstone depositional environment, further evidence must be found to ascertain an eolian origin for the Mt. Simon.

4) Quantitative heavy mineral studies indicate that rounded to subrounded zircon, tourmaline, garnet and rutile are the most abundant detrital non-opaque heavy minerals. Minor quantities (<2.4 percent total) of diaspore, anatase (authigenic), apatite, amphibole, epidote, staurolite and pyroxene are also present. The most common opaque heavy minerals are pyrite, magnetite and hematite.

5) A ZTRG index is proposed (modified from the original ZTR index of Hubert, 1962), as the percentage of zircon, tourmaline, rutile and garnet among the non-opaque, non-micaceous detrital heavy mineral fraction in a sandstone.

7) ZTRG indices above 95.7 (except in two of eleven samples) indicate a high mineralogical maturity of the sandstones. The question of whether the high maturity results from the elimination of labile constituents during transport or is the result of recycling from older sandstones cannot be answered clearly using petrographic observations. The fact that the most common heavy minerals (zircon, tourmaline and garnet), which are highly resistant to abrasion (hardnesses between 6.5 and 7.5) and chemically stable, are usually rounded whereas quartz (also highly resistant with a hardness of 7 and chemically stable) in the same size fraction is usually subrounded to subangular, could support the thesis that the sandstones are the product of recycling of older sediments. A wide variety of Precambrian source rocks were available during Mt. Simon time. Perhaps part of the Mt. Simon Sandstone was derived from older Precambrian sandstones and the other part is the result of extensive abrasion of first cycle detritus in high energy environments.

8) Ojakangas (1963) showed evidence of Precambrian sedimentary sources for the Upper Cambrian Lamotte Sandstone in Missouri which is correlative with the Upper Cambrian Mt. Simon Sandstone in Minnesota. Some of these lines of evidence are also present in the Mt. Simon, includng: a) an ultrastable mineralogy represented by submature to mature quartzose sandstones containing sub-rounded to well-rounded quartz, zircon, tourmaline, rutile and garnet; b) the presence in the Lake Superior region of tourmaline-bearing Precambrian sandstones, and c) the paleoslope dipping toward the south. Several highlands around the Hollandale embayment were logical sources of sediments for the Mt. Simon. The Sioux Quartzite represents a direct source for rocks in the western part of the embayment. Other possible sources around the embayment include rocks from the Transcontinental arch toward the northwest, volcanic and sedimentary rocks of the Midcontinent Rift System to the north but also underlying the embayment, and rocks from the Wisconsin dome and the Wisconsin arch to the northeast and east of the embayment. The most likely Precambrian sedimentary units that could have been sources for the Mt. Simon are the Hinckley Sandstone, the Fond du Lac and Solor Church Formations, the Bayfield Group of Wisconsin, and the already mentioned Sioux Quartzite.

9) Petrographic analyses of the Mt. Simon Sandstone has shown it to contain an average of 15 percent in volume of cement and 15.5 percent pore space. The most abundant authigenic mineral is K-feldspar which is present as euhedral overgrowths on detrital feldspar grains. Other authigenic minerals in the unit include quartz, carbonates (calcite, dolomite and siderite ?), kaolinite, illite, pyrite, hematite and leucoxene.

10) Evidence for the formation of authigenic feldspar in the unit are not conclusive. According to Kastner and Siever (1979) the unmetamorphosed character of the host sediments and the properties of the feldspars themselves could indicate a low to moderate temperature origin. The occurrence of authigenic feldspar could fit either the isochemical or the mass transfer models proposed by the above mentioned authors. The connection between alkaline-hypersaline systems and the formation of authigenic K-feldspar as proposed by Long and Lyons (1992) should not be ruled out for the Mt. Simon Sandstone.

11) The diagenetic history of the Mt. Simon Sandstone can be divided into three stages: A) An early diagenesis stage represented by precipitation of leucoxene (titanium oxide) and iron oxides (hematite and limonite/goethite); B) A burial diagenesis stage marked by the precipitation of quartz, potassium feldspar, kaolinite, illite (?), dolomite and siderite (?); and C) A late diagenesis stage with calcite and pyrite replacing most of the previous cements and filling pore spaces.

12) Several samples show evidence of dissolution porosity in thin section (secondary porosity). Petrographic clues to the presence of secondary pores in the Mt. Simon Sandstone include oversized pores, intragranular pores (partially dissolved detrital grains), and partially dissolved cements and matrix. Minerals that were dissolved include feldspars, dolomite, and glauconite.

REFERENCES CITED

ALEINIKOFF, J.N., WALTER, M., KUNK, M.J., AND HEARN, P.P. Jr., 1993. Do ages of authigenic K-feldspar date formation of Mississippi Valley-type Pb-Zn deposits, central and southeastern United States?: Pb isotopic evidence: Geology, v. 21, p. 73-76.

ASTHANA, V., 1969. The Mt. Simon Formation (Dresbachian stage) of Wisconsin: Unpublished Ph.D. thesis. University of Wisconsin, Madison, 159 p.

AUSTIN, G.S., 1969. Paleozoic lithostratigraphic nomenclature for southeastern Minnesota: Minnesota Geological Survey Information Circular 6, 11 p.

AUSTIN, G.S., 1970. Deep stratigraphic test well near Hollandale, Minnesota: Minnesota geological survey Report of Investigations 12, 52 p.

AUSTIN, G.S., 1972. Paleozoic lithostratigraphy of southeastern Minnesota: In: Sims, P.K., and Morey, G.B., Eds. Geology of Minnesota: A Centennial Volume: Minnesota Geological Survey, p. 459-473.

BASKIN, Y., 1956. A study of authigenic feldspars: Journal of Geology, v. 64, p. 132-155.

BJØRLYKKE, K., 1983. Diagenetic reactions in sandstones: In: Sediment Diagenesis, Ed. by A. Parker and B.W. Sellwood. NATO ASI Series C, Mathematical and Physical Sciences, v. 115, p. 169-213.

BLATT, H., 1992. Sedimentary petrography; second edition: New York, W. H. Freeman and Company, 514 p.

BUNKER, B.J., WITZKE, B.J., WATNEY, W.L., AND LUDVIGSON, G.A., 1988. Phanerozoic history of the central midcontinent, United States: In: Sloss, L.L., ed., Sedimentary Cover-North American, Craton: U.S.A. Geological Society of America, The Geology of North America, v. D-2, p. 243-260.

BURLEY, S.D., KANTOROWICZ, J.D. AND WAUGH, B., 1985. Clastic diagenesis: In: Sedimentology, Recent developments and applied Aspects (Ed. by P.J. Brenchley and B.P. Williams). Spec. publ. Geol. Soc. London, 18, p. 189-226.

CAROZZI, A.V., 1993. Sedimentary petrography: New Jersey, PTR Prentice Hall, 263 p.

COTTINGHAM, J.T., 1990. Cambrian/Early Ordovician sequence stratigraphy and Mt. Simon Sandstone petrology-Michigan basin. [Abs]: American Association of Petroleum Geologists Bulletin, v. 74, p. 634.

DEER, W.A., HOWIE, R.A., AND ZUSSMAN, J., 1992. An introduction to the rock forming minerals, second edition: Honk Kong, Longman Scientific and technical, 696 p.

DEMING, D., 1992. Catastrophic release of heat and fluid flow in the continental crust: Geology, v. 60, p. 235-239.

DRIESE, S.G., BYERS, C.W., AND DOTT, R.H. Jr., 1981. Tidal Deposition in the basal Upper Cambrian Mt. Simon Formation in Wisconsin: Journal of Sedimentary Petrology, v. 51, p. 367-381.

DUFFIN, M.E., LEE, M.C., KLEIN, G. dev, AND HAY, R.L., 1989. Potassic diagenesis of Cambrian sandstones and Precambrian granitic basement in UPH-3 deep hole, Upper Mississippi Valley, U.S.A: Journal of Sedimentary petrology, v. 59, p. 848-861.

DUFFIN. M. E., 1990. Potassic alteration of Cambrian-Ordovician sandstones and Precambrian basement rocks of the North American Midcontinent: Unpublished Ph.D. Thesis. University of Illinois, Urbana-Champaign, 121 p.

DUNOYER De SEGONZAC, G., 1968. The birth and development of the concept of diagenesis (1866-1966): Earth Science Reviews, v. 4, p. 153-201.

FISHMAN, N.S., 1992. Diagenetic studies of the Mt. Simon Sandstone-Implications for paleohydrology: U.S. Geological Survey open file report OF 92-0001, p. 11-12.

GOLDICH, S.S., 1934. Authigenic feldspar in sandstones of Southeastern Minnesota: Journal of Sedimentary Petrology, v. 4, p. 89-95.

GRAHAM, W.A.P., 1930. A textural and petrographic study of the Cambrian sandstones of Minnesota: Journal of Geology, v. 38, p. 696-716.

HEALD, M.T., AND LARESE, R.E., 1973. The significance of the solution of feldspar in porosity development: Journal of Sedimentary Petrology, v. 43, p. 458-460.

HEALD, M.T., AND BAKER G.F., 1979. Diagenesis of the Mt. Simon and Rose Run Sandstones in western West Virginia and southern Ohio: Diagenesis of Sandstone: Cement - Porosity relationships, SEPM reprint series number 9, p. 154-165.

HEARN, P.P. Jr., AND SUTTER, J.F., 1985. Authigenic potassium feldspar in Cambrian carbonates: Evidence of Alleghanian brine migration: Science, v. 228, p. 1529-1531.

HEARN, P.P, Jr., SUTTER, J.F., AND BELKIN, H.E., 1987. Evidence for Late-Paleozoic brine migration in Cambrian carbonate rocks of the central and southern Appalachians: Implications for Mississippi Valley-type sulfide mineralization: Geochimica et Cosmochimica Acta, v. 51, p. 1323-1334.

HEARN, P.P. Jr., GANDY, J.D., ALEINIKOFF, J.N., AND WERRE, R.W., 1989. Separation of authigenic overgrowths from mineral grains by air-abrasion and gravity settling techniques: In: New frontiers in stable isotopic research, United States Geological Survey Bulletin 1890, p. 111-115.

HOHOLICK, J.D., METARKO, T., AND POTTER, P.E., 1984. Regional variations of porosity and cement: St. Peter and Mt. Simon sandstones in Illinois Basin: American Association of Petroleum Geologists Bulletin, v. 68, p. 753-764.

HUBERT, J.F., 1962. A zircon-tourmaline-rutile maturity index and the interdependence of the composition of heavy mineral assemblages with the gross composition and texture of sandstones: Journal of Sedimentary Petrology, v. 32, p. 440-450.

KASTNER, M., 1971. Authigenic feldspars in carbonate rocks: American Mineralogist, v. 56, p. 1403-1442.

KASTNER, M., AND SIEVER, R., 1979. Low temperature feldspars in sedimentary rocks: American Journal of Science, v. 279, p. 435-479.

KIESTER, S.A., 1976. The mineralogy and sedimentology of the Cambrian strata of southeastern Minnesota: Unpublished M.S. thesis, Northern Illinois University, Dekalv, Illinois. 76 P.

LEACH, D.L., AND ROWAN, E.L., 1986. Genetic link between Ouachita foldbelt tectonism and the Mississippi Valley-type lead-zinc deposits of the Ozarks: Geology, v. 14, p. 931-935.

LOCHMAN-BALK, C., 1970. Upper Cambrian faunal patterns on the craton: Geological Society of America Bulletin, v. 81, p. 3197-3224.

LONG, D.T., AND LYONS, W.B., 1992. Aridity, continental weathering, and ground-water chemistry: GSA Today v. 2, p. 185-186 and 188-190.

MARSHALL, B.D., WOODARD, H.H., AND DePAOLO, D.J., 1986. K-Ca-Ar systematics of authigenic sanidine from Waukau, Wisconsin, and the diffusivity of argon: Geology, v. 14, p. 936 - 938.

METARKO, T.A., 1980. Porosity, water chemistry, cement and grain fabric with depth in the Upper Cambrian Mount Simon and Lamotte Sandstones: [Unpub. M.S. thesis], University of Cincinnati, Ohio, 79 p.

MOSSLER, J.H., 1987. Paleozoic lithostratigraphic nomenclature for Minnesota: Minnesota Geological Survey, Report of investigations 36, 36 p.

MOSSLER, J.H., 1992. Sedimentary rocks of Dresbachian age (Late Cambrian), Hollandale Embayment, Southeastern Minnesota: Minnesota Geological Survey Report of Investigations 40, 71 p.

ODOM, I.E., 1974. Syngenetic sanidine beds from Middle Ordovician Saint Peter Sandstone, Wisconsin: A discussion: Journal of Geology, v. 82, p. 112-116.

ODOM, I.E., 1975. Feldspar grain-size relations in Cambrian arenites, Upper Mississippi Valley: Journal of Sedimentary Petrology, v. 45, p. 636-650.

ODOM, I.E., DOE, T.W., AND DOTT, R.H., Jr., 1976. Nature of feldspar-grain size relations in some quartz-rich sandstones: Journal of Sedimentary Petrology, v. 46, p. 862-870.

OJAKANGAS, R.W., 1963. Petrology and sedimentation of the Upper Cambrian Lamotte Sandstone in Missouri: Journal of Sedimentary Petrology, v. 33, p. 860-873

OLIVER, J., 1986. Fluids expelled tectonically from orogenic belts: Their role in hydrocarbon migration and other geological phenomena: Geology, v. 14, p. 99-102.

PETTIJOHN, F.J., POTTER, P.E., AND SIEVER, R., 1987. Sand and Sandstone, second edition: New York, Springer Verlag, 553 p.

SCHMIDT, V., AND McDONALD D.A., 1979. Secondary reservoir porosity in the course of sandstone diagenesis: American Association of Petroleum Geologists, Education coarse note series No. 12, 125 p.

SCHOLLE, P.A., 1981. A color illustrated guide to constituents, textures, cements, and porosities of sandstones and associated rocks: American Association of Petroleum Geologists Memoir 28, 200 p.

STABLEIN, N.K., III, AND DAPPLES, E.C., 1977. Feldspars of the Tunnel City Group (Cambrian), western Wisconsin: Journal of Sedimentary Petrology, v. 47, p. 1512-1538.

TESTER, A.C., AND ATWATER, G.I., 1934. The occurrence of authigenic feldspars in sediments: Journal of Sedimentary Petrology, v. 4, p. 23-31.

VAN STRAATEN, L.M.J.U., 1948. Note on the occurrence of authigenic feldspar in non-metamorphic sediments: American Journal of Science, v. 246, p. 569-572.

WALKER, T.R., 1984. 1984 SEPM Presidential address: Diagenetic albitization of potassium feldspar in arkosic sandstones: Journal of Sedimentary Petrology, v. 54, p. 3-16.

WEBERS, G.F., 1972, Paleoecology of the Cambrian and Ordovician strata of Minnesota: In: Sims, P.K., and Morey, G.B., Eds. Geology of Minnesota: A Centennial Volume: Minnesota Geological Survey, p. 474-484.

WOODARD, H.H., 1972. Syngenetic sanidine beds from Middle Ordovician Saint Peter Sandstone, Wisconsin: Journal of Geology, v. 80, p. 323-332.

WOODARD, H.H., 1974. Syngenetic sanidine beds from Middle Ordovician Saint Peter Sandstone, Wisconsin: A reply: Journal of Geology, v. 82, p. 116-119.

ZOLTAI, T., AND STOUT, J.H., 1984. Mineralogy concepts and principles: Minneapolis, Burgess Publishing Company, 505 p.

APPENDIX I

List of references relevant to feldspar authigenesis in sandstones. References are arranged in chronological order.

ALEINIKOFF, J.N., WALTER, M., KUNK, M.J., AND HEARN, P.P. Jr., 1993. Do ages of authigenic K-feldspar date formation of Mississippi Valley-type Pb-Zn deposits, central and southeastern United States?: Pb isotopic evidence: Geology, v. 21, p. 73-76.

CAROZZI, A.V., 1993. Sedimentary Petrography, PTR Prentice Hall, New Jersey, 263 p.

LONG, D.T., and LYONS, W.B., 1992. Aridity, Continental Weathering, and Ground-Water Chemistry: GSA Today v. 2, p. 185-186 and 188-190.

WORDEN, R. H., AND RUSHTON, J.C., 1992. Diagenetic K-feldspar Textures: A TEM study and model for diagenetic feldspar growth: Journal of Sedimentary Petrology, v. 62, p. 779-789.

DUFFIN. M. E., 1990. Potassic alteration of Cambrian-Ordovician sandstones and Precambrian basement rocks of the North American Midcontinent: Unpublished Ph.D. Thesis. University of Illinois, Urbana-Champaign, 121 p.

DIEHL, S.F., GOLDHABER, M.B., AND MOSIER, E.L., 1990. Regions of feldspar precipitation and dissolution in the Lamotte Sandstone, Missouri - implications for MVT ore genesis: U.S. Geological Survey Circular 1043, p. 4-5.

HEARN, P.P. Jr., GANDY, J.D., ALEINIKOFF, J.N., AND WERRE, R.W., 1989. Separation of authigenic overgrowths from mineral grains by air-abrasion and gravity settling techniques: In: New frontiers in stable isotopic research, United States Geological Survey Bulletin 1890, p. 111-115.

KRAINER, K., AND SPÖTL, C., 1989. Detrital and authigenic feldspars in Permian and early Triassic sandstones, Eastern Alps (Austria): Sedimentary Geology., v. 62, p. 59-77.

DUFFIN, M.E., LEE, M.C., KLEIN, G. dev, AND HAY, R.L., 1989. Potassic diagenesis of Cambrian sandstones and Precambrian granitic basement in UPH-3 deep hole, Upper Mississippi Valley, U.S.A: Journal of Sedimentary petrology, v. 59, p. 848-861.

DUFFIN, M.E., 1989. Nature and origin of authigenic K-feldspar in Precambrian basement rocks of the North American midcontinent: Geology, v. 17, p. 756-768.

MILLIKEN, K.L., 1989. Petrography and composition of authigenic feldspars, Oligocene Frio Formation, South Texas: Journal of Sedimentary Petrology, v. 59, p. 361-374.

LEE, M., AND ARONSON, J.L., 1988. Multiple episodes of potassic diagenesis of Paleozoic sandstones and tuffs in the Upper Mississippi Valley mineral district.[Abs]: Geological Society of America Abstracts with programs, v. 20 p.354.

HAY, R.L., LEE, M., KOLATA, D.R., MATTHEWS, J.C., AND MORTON, J.P., 1988. Episodic potassic diagenesis of Ordovician tuffs in the Mississippi Valley area: Geology, v. 16, p. 743-747.

BJØRKUM, P.A., AND GJELSVIK, N., 1988. An isochemical model for formation of authigenic kaolinite, K-feldspar and illite in sediments: Journal of Sedimentary Petrology, v. 58, p. 506-511.

HEARN, P.P. Jr., 1987. A quantitative technique for determining the mass-fractions of authigenic and detrital K-feldspar in mineral separates: Scanning Microscopy, v. 1, p. 1039-1043.

GOLD, P.B., 1987. Textures and geochemistry of authigenic albite from Miocene sandstones, Louisiana Gulf Coast: Journal of Sedimentary Petrology, v. 57, p. 353-362.

MCBRIDE, E.F., LAND, L.S., AND MACK, L.E., 1987. Diagenesis of eolian and fluvial feldspathic sandstones, Norphlet Formation (Upper Jurassic), Rankin County, Mississippi, and Mobile County, Alabama: The American Association of Petroleum Geologists Bulletin, v. 71, p. 1019-1034.

PETTIJOHN, F.J., POTTER, P.E., AND SIEVER, R., 1987. Sand and Sandstone, second edition. Springer-Verlag, New York, 553 p.

MARSHALL, B.D., WOODARD, H.H., AND DePAOLO, D.J. 1986. K-Ca-Ar systematics of authigenic sanidine from Waukau, Wisconsin, and the diffusivity of argon: Geology, v. 14, p. 936-938.

HEARN, P.P. Jr., LINDHOLM, R.C., AND SUTTER, J.F., 1986. Authigenic potassium feldspar in ribbon rocks of the Cambrian-Conococheague Limestone, Western Maryland. In: F.A. Mumpton (Editor), Studies in diagenesis. U.S. Geological Survey Bulletin 1578, p. 183-196.

WALKER, T.R., 1984. 1984 SEPM Presidential address: Diagenetic albitization of potassium feldspar in arkosic sandstones: Journal of Sedimentary Petrology, v. 54, p. 3-16.

ALI, A.D., AND TURNER, P., 1982. Authigenic K-Feldspar in the Bromsgrove Sandstone Formation (Triassic) of Central England: Journal of Sedimentary Petrology, v. 52, p. 187-197.

LAND, L.S., AND MILLIKEN, K.L., 1981. Feldspar diagenesis in the Frio Formation, Brazoria County, Texas Gulf Coast: Geology, v. 9, p. 314-318.

KASTNER, M., AND SIEVER, R., 1979. Low temperature feldspars in sedimentary rocks: American Journal of Science, v. 279, p. 435-479.

WAUGH, B., 1978. Authigenic K-feldspar in British Permo-Triassic sandstones: Journal Geological Society of London, v. 135, p. 51-56.

SIBLEY, D.F., 1978. K-feldspar cement in the Jacobsville Sandstone: Journal of Sedimentary Petrology, v. 48, p. 983-986.

STABLEIN, N.K., III, AND DAPPLES, E.C., 1977. Feldspars of the Tunnel City Group (Cambrian), western Wisconsin: Journal of Sedimentary Petrology, v. 47, p. 1512-1538.

ODOM, I.E., DOE, T.W., AND DOTT, R.H., Jr., 1976. Nature of feldspar-grain size relations in some quartz-rich sandstones: Journal of Sedimentary Petrology, v. 46, p. 862-870.

BUYCE, M.R., AND FRIEDMAN, G.M., 1976. Significance of authigenic K-feldspar in Cambrian-Ordovician carbonate rocks of the Proto-Atlantic shelf in North America: Reply to discussion and new data: Journal of Sedimentary Petrology, v. 46, p. 1039-1040.

MAZZULLO, S.J., 1976. Significance of authigenic K-feldspar in Cambrian-Ordovician carbonate rocks of the Proto-Atlantic shelf in North America: A discussion: Journal of Sedimentary Petrology, v. 46, p. 1035-1040.

BUYCE, M.R., AND FRIEDMAN, G.M., 1975. Significance of authigenic K-feldspar in Cambrian-Ordovician carbonate rocks of the Proto-Atlantic shelf in North America: Journal of Sedimentary Petrology, v. 45, p. 808-821.

ODOM, I.E., 1975. Feldspar grain-size relations in Cambrian arenites, Upper Mississippi Valley: Journal of Sedimentary Petrology, v. 45, p. 636-650.

DESBOROUGH, G.A., 1975. Authigenic albite and potassium feldspar in the Green River Formation, Colorado and Wyoming: American Mineralogist, v. 60, p. 235-239.

WOODARD, H.H., 1974. Syngenetic sanidine beds from Middle Ordovician Saint Peter Sandstone, Wisconsin: A reply: Journal of Geology, v. 82, p. 116-119.

ODOM, I.E., 1974. Syngenetic sanidine beds from Middle Ordovician Saint Peter Sandstone, Wisconsin: A discussion: Journal of Geology, v. 82, p. 112-116.

HEALD, M.T., AND LARESE, R.E., 1973. The significance of the solution of feldspar in porosity development: Journal of Sedimentary Petrology, v. 43, p. 458-460.

WOODARD, H.H., 1972. Syngenetic sanidine beds from Middle Ordovician Saint Peter Sandstone, Wisconsin: Journal of Geology, v. 80, p. 323-332.

GLOVER, J.E., AND HOSEMANN P., 1970. Optical data on some authigenic feldspars from Western Australia: Mineralogical magazine, v. 37, p. 588-592.

GOVINDA RAO SINDHIA, M.R., AND VISWANATHIAH, M.N., 1968. Occurrence of authigenic feldspars in arkosic sandstones of Kaladgi formations, Badami, Mysore State, India: Journal of Sedimentary Petrology, v.38, p. 1344-1347.

GOVINDA RAJULU B.V., AND NAGARAJA, H.R., 1967. Authigenic feldspars from the lower Kaladgi arkoses of Jamkhandi, Mysore State, India: Journal of Sedimentary Petrology, v. 37, p. 707-709.

BASKIN, Y., 1956. A study of authigenic feldspars: Journal of Geology, v. 64, p.132-155.

BERG, R.R., 1952. Feldspathized sandstone: Journal of Sedimentary Petrology, v. 22, p. 221-223.

VAN STRAATEN, L.M.J.U., 1948. Note on the occurrence of authigenic feldspar in non-metamorphic sediments: American Journal of Science, v. 246, p. 569-572.

GOLDICH, S.S., 1934. Authigenic feldspar in sandstones of Southeastern Minnesota: Journal of Sedimentary Petrology, v. 4, p. 89-95.

TESTER, A.C., AND ATWATER, G.I., 1934. The occurrence of authigenic feldspars in sediments: Journal of Sedimentary Petrology, v. 4, p. 23-31.